PLOS ONE

Curcumin improves D-galactose and normal-aging associated memory impairment in mice: In vivo and in silico-based studies

Md. Ashrafur Rahman[1,2]*, Arif Anzum Shuvo[1], Asim Kumar Bepari[1], Mehedi Hasan Apu[1], Manik Chandra Shill[1], Murad Hossain[1], Mohammed Uddin[3,4], Md. Rabiul Islam[5], Monjurul Kader Bakshi[1], Javed Hasan[1], Atiqur Rahman[1], Ghazi Mohammad Sayedur Rahman[1], Hasan Mahmud Reza[1]*

1 Department of Pharmaceutical Sciences, North South University, Bashundhara, Dhaka, Bangladesh, 2 Department of Pharmaceutical Sciences, Jerry H. Hodge School of Pharmacy, Texas Tech University Health Science Center (TTUHSC), Amarillo, TX, United States of America, 3 College of Medicine, Mohammed Bin Rashid University of Medicine and Health Sciences, Dubai, UAE, 4 Cellular Intelligence (Ci) Lab, GenomeArc Inc., Toronto, ON, Canada, 5 Department of Pharmacy, University of Asia Pacific, Dhaka, Bangladesh

* ashrafurrahman82@gmail.com (MAR); hasan.reza@northsouth.edu (HMR)

Abstract

Aging-induced memory impairment is closely associated with oxidative stress. D-Galactose (D-gal) evokes severe oxidative stress and mimics normal aging in animals. Curcumin, a natural flavonoid, has potent antioxidant and anti-aging properties. There are several proteins like glutathione S-transferase A1 (GSTA1), glutathione S-transferase omega-1 (GSTO1), kelch-like ECH-associated protein 1 (KEAP1), beta-secretase 1 (BACE1), and amine oxidase [flavin-containing] A (MAOA) are commonly involved in oxidative stress and aging. This study aimed to investigate the interaction of curcumin to these proteins and their subsequent effect on aging-associated memory impairment in two robust animal models: D-Gal and normal aged (NA) mice. The aging mice model was developed by administering D-gal intraperitoneally (i.p). Mice (n = 64) were divided into the eight groups (8 mice in each group): Vehicle, Curcumin-Control, D-gal (100mg/kg; i.p), Curcumin + D-gal, Astaxanthin (Ast) + D-gal, Normal Aged (NA), Curcumin (30mg/kg Orally) + NA, Ast (20mg/kg Orally) + NA. Retention and freezing memories were assessed by passive avoidance (PA) and contextual fear conditioning (CFC). Molecular docking was performed to predict curcumin binding with potential molecular targets. Curcumin significantly increased retention time (p < 0.05) and freezing response (p < 0.05) in PA and CFC, respectively. Curcumin profoundly ameliorated the levels of glutathione, superoxide dismutase, catalase, advanced oxidation protein products, nitric oxide, and lipid peroxidation in mice hippocampi. In silico studies revealed favorable binding energies of curcumin with GSTA1, GSTO1, KEAP1, BACE1, and MAOA. Curcumin improves retention and freezing memory in D-gal and nature-induced aging mice. Curcumin ameliorates the levels of oxidative stress biomarkers in mice. Anti-aging effects of curcumin could be attributed to, at least partially, the upregulation of antioxidant enzymes through binding with GSTA1, GSTO1, KEAP1, and inhibition of oxidative damage through binding with BACE1 and MAOA.

1. Introduction

Aging is a natural process characterized by gradual deterioration in diverse physiological functions [1], including oxidative damage-driven memory loss [2]. Memory dysfunction could be triggered by an imbalance among reactive oxygen species (ROS), reactive nitrogen species (RNS), and antioxidant enzyme activities [3]. The excess generation of ROS, RNS, and reduction in antioxidant enzyme activities in the brain escalate lipid peroxidation, protein oxidation, and mitochondrial DNA (mtDNA) damage [4], contributing to brain aging [5]. Brain aging and accompanied cognitive dysfunction are typical features of neurodegenerative diseases [6]. One study claimed that D-galactose (D-gal) accelerates the brain-aging process in animal models similar to the normal aging in humans [7]. D-gal-induced aging mice model has gained popularity among researchers because of its feasibility, fewer side effects, and higher survival rate of animals. It was reported that D-gal evokes aging-induced memory impairment through neurodegeneration, aberrant immune responses, and abnormal gene expression [8]. Another study suggests that D-gal increases malondialdehyde (MDA) level and decreases the antioxidant enzymes such as superoxide dismutase (SOD) and glutathione (GSH) [9]. At high doses, D-gal can accelerate cellular ROS generation through multiple mechanisms, such as adenosine triphosphate (ATP) depletion, redox homeostasis impairment, and elevation of the advanced glycation end product (AGE), the receptor for the advanced glycation end product (RAGE), and nicotinamide adenine dinucleotide phosphate (NADPH) oxidase [10]. Overproduction of ROS induces oxidative stress, cellular apoptosis, inflammation, and mitochondrial dysfunction, which leads to neuronal degeneration [11]. Raised free radical levels were implicated in cholinergic neuron dysfunctions in the brain [12] and aging-associated memory impairment [13]. Currently, several acetyl-cholinesterase (AChE) inhibitors (donepezil, rivastigmine, and galantamine) and an N-Methyl-D-aspartate (NMDA) receptor antagonists (memantine) are used in aging-associated memory impairment. The outcome of the treatment has not reached the optimum level owing to side effects and cost-ineffectiveness. Studies showed that natural compounds could be a promising solution for aging-associated memory impairment due to their antioxidants, anti-inflammatory, and anti-aging properties [14]. Furthermore, plant-derived compounds can be a choice on account of their cost-effectiveness. Curcumin, a natural compound found in Curcuma Longa, is regularly used as spicey ingredients and possesses anti-inflammatory, antioxidant, and anti-aging properties [15] by regulating several proteins such as tumor necrosis factor alpha (TNFα) [16], mammalian target of rapamycin (mTOR), sirtuin, and adenosine monophosphate-activated protein kinase (AMPK) [17]. However, several proteins like glutathione S-transferase A1 (GSTA1), glutathione S-transferase omega-1 (GSTO1), kelch-like ECH-associated protein 1 (KEAP1), beta-secretase 1 (BACE1), and amine oxidase [flavin-containing] A (MAOA) are commonly involved in oxidative stress and aging [18]. GSTA1 regulates GSH conjugation, which may reduce oxidative stress [19]. Another protein, GSTO1, modulates conjugation of GSH [19], the activation of interleukin-1β, and inflammation in aging-associated neurodegenerative disease [20]. KEAP1 plays an antioxidative role by regulating the Nrf2 cytoprotective signaling pathway [21]. BACE1 is closely associated with the generation of β-amyloid (Aβ) in aging-induced neurological disease, Alzheimer's Disease [22]. Overproduction of MAOA in the brain triggers oxidative overload [23]. However, no study has detected the interaction of curcumin with antioxidant and aging regulating proteins GSTA1, GSTO1, KEAP1, BACE1, MAOA and their consequent impact on improving the memory. Therefore, it would be interesting to find the binding affinity of curcumin with these proteins in order to determine their subsequent impacts on modulating the oxidative biomarkers in the aging process. We have extensively

investigated the effects of curcumin on two robust animal models; the normal aging and the D-gal induced aged mice model, using two widely acceptable behavioral tasks: passive avoidance (PA) and contextual fear conditioning (CFC). We also biochemically assayed the levels of oxidative stress biomarkers, including glutathione (GSH), superoxide dismutase (SOD), catalase (CAT), advanced oxidation of protein products (AOPP), nitric oxide (NO), and malondialdehyde (MDA) in mice hippocampi. Moreover, we performed in silico analysis to illustrate the binding of curcumin with protein molecules implicated in brain oxidative stress pathophysiologies. Overall, this study has comprehensively discerned the effects of curcumin on aging-related memory impairment by a battery of behavioral, biochemical, and molecular docking experiments.

2. Materials and methods

2.1. In vivo

2.1.1. Chemicals. Curcumin, D-gal, Ast, and thiobarbituric acid (TBA) trichloroacetic acid (TCA) were purchased from Sigma-Aldrich (Germany). All other chemicals, reagents, and solvents used in this study were analytical grade.

2.1.2. Experimental animals. We used randomly selected healthy male *Swiss albino* mice in this study. We chose male mice because of their tendency in increasing context fear expression toward adulthood, unlike female mice [24]. Forty adult male mice (40 ± 2 gm; 6–8 weeks) were divided into four groups, and 24 normal-aged mice (42 ± 2 gm; 10–12 months) were divided into three groups. Each group consisted of eight mice. Mice were reared at 25˚C temperature, 55% ± 15% relative humidity, 12:12 hours light-dark cycle with an adequate supply of food pellets and pure drinking water.

2.1.3. Preparation of drugs. Curcumin was suspended in 0.25% w/v sodium carboxymethylcellulose and administered at a 1ml/100g body weight [25]. D-gal was prepared freshly by dissolving in 0.9% of saline before each session [26]. Ast powder was dissolved in distilled water at the ratio of 20mg/20ml [27].

2.1.4. Experimental design. We divided sixty-four mice into the following eight groups (Each group consisted of eight mice):

1. Vehicle (n = 8): 0.25% w/v sodium carboxymethylcellulose was administered (oral gavage) [25] once daily for ten weeks.

2. Curcumin-Control (Positive Control; n = 8): Curcumin 30mg/kg [25] was administered orally (oral gavage) once daily for ten weeks.

3. D-gal (n = 8): D-gal (100mg/kg) was administered intraperitoneally [26] once daily for ten weeks.

4. Curcumin + D-gal (n = 8): Curcumin 30mg/kg [25] and D-gal 100mg/kg [26] were administered orally (oral gavage) and intraperitoneally, respectively, once daily for ten weeks.

5. Ast (standard antioxidant) + D-gal (n = 8): Ast 20mg/kg [28, 29] and D-gal 100mg/kg [26] were administered orally (oral gavage) and intraperitoneally, respectively once daily for ten weeks.

6. NA (n = 8): Normal mice pellets and water was given daily throughout the experiment.

7. Curcumin + NA (n = 8): Curcumin 30mg/kg was given orally (oral gavage) [25] once daily for ten weeks.

8. Ast (standard antioxidant) + NA (n = 8): Ast (20mg/kg) was administered orally (oral gavage) [28, 29] once daily for ten weeks.

After ten weeks of treatment, we investigated retention and freezing memory by PA and CFC tests, respectively. The animals were then euthanized for collecting brain tissues to assay oxidative stress biomarkers. Finally, the molecular targets of curcumin were assessed by in silico analysis (Fig 1).

2.1.5. Passive avoidance test. The method of PA was performed as demonstrated by Tabrizian [30]. The PA behavior study was executed with a step-through type avoidance learning task that calculates the memory retention of mice. This test consisted of three sessions. Firstly, each mouse was placed gently in the experimental apparatus in the habituation session and allowed to habituate for at least 5 minutes on day 1. Mice that did not enter into the dark chamber after keeping them in a light chamber for more than 120 s were excluded from the experiment. Secondly, the training session was used to evaluate the learning and exploration. This session consisted of 3 trials with 30 min intervals. In the first trial, each mouse was gently placed in the light, and the sliding door was opened after 10 seconds. Each mouse was allowed to explore both chambers for 5 minutes. Each mouse's time before entering the dark chamber with all four paws was recorded as the retention period (300 s was considered a cut-off point). The second trial was performed in a similar way to the first trial. In the third trial, once a mouse stepped through the dark chamber with all four paws, the sliding door was closed. An electrical foot shock (0.3–0.5 mA for 2 s) was delivered. After the foot shock, each mouse was kept in the dark chamber for an additional 10 s to build an association between chambers and the foot shock, and then the mouse was returned to the home cage. Repeated training was conducted similarly for five consecutive days with 24 hours intervals. The objective of this testing session was to determine memory RT after 24 and 48 hours of training. No electrical foot-
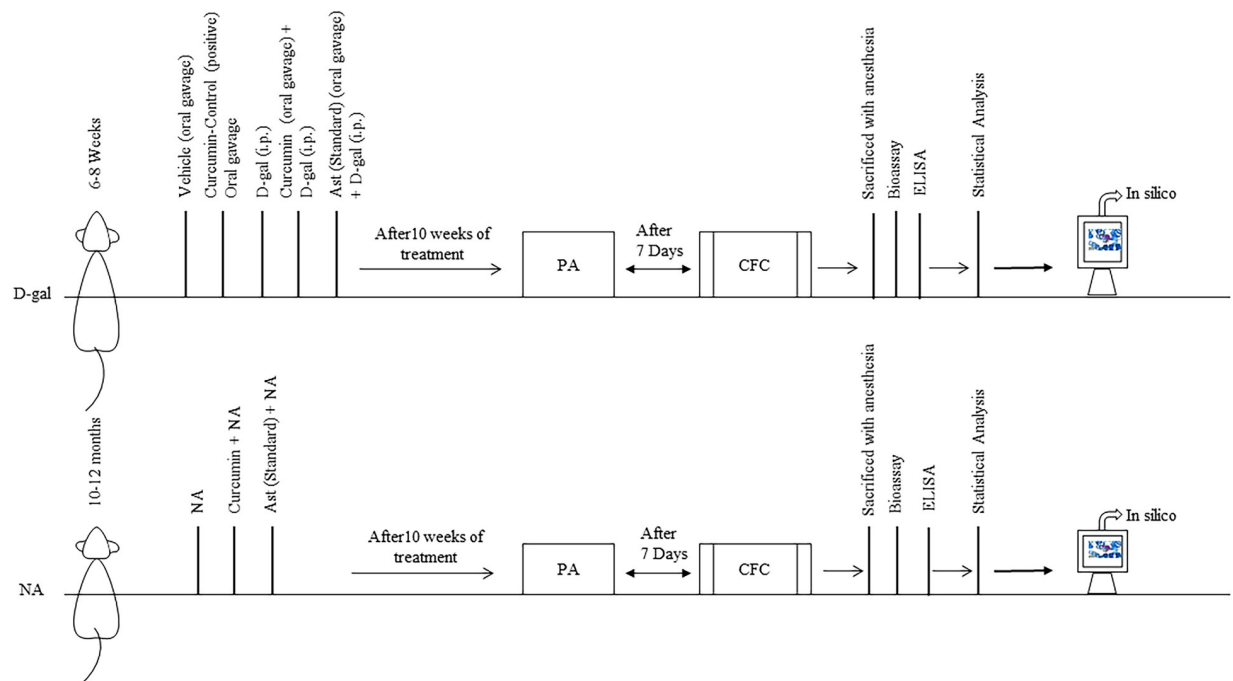
Fig 1. Schematic diagram of total experimental procedures: The treatment was continued for ten weeks. After that, the behavioral tests were performed using Passive Avoidance (PA) and Contextual Fear Conditioning (CFC). The biomarkers were detected after completing the behavioral tasks. In-silico studies were used to determine curcumin's binding affinity to targeted proteins.

https://doi.org/10.1371/journal.pone.0270123.g001

shock was applied during this session. The retention period was measured using a stopwatch. The apparatus was adequately cleaned with 70% ethanol before the experiment.

2.1.6. Contextual fear conditioning test. The CFC Test was performed after seven days of completion of the PA test. The method of CFC was performed as demonstrated by Shoji [31]. In brief, each mouse was placed in a transparent acrylic chamber (33 × 25 × 28 cm) with a stainless-steel grid floor (0.2 cm diameter, spaced 0.5 cm apart; O'Hara & Co., Tokyo, Japan) and was allowed to navigate independently for 2 min. Next, the conditioned stimulus (CS) of 55 dB white noise was presented for 30 s. During the last 2 s of CS presentation, the unconditioned stimulus (US) of a mild foot shock (0.3 mA, 2 s) was applied. Two more CS-US pairings were presented with a 2-min inter-stimulus interval. A context test was conducted to detect contextually conditioned fear memory in the same chamber approximately 24 hours (2a) and 30 days (31a) after the conditioning session. A cued test was performed to detect a novel fear memory in an altered context. The cued test was conducted in a triangular chamber (33 × 29 × 32 cm) made of opaque white plastic located in a different room. The test was done a few hours after the context test on day 2 (2b) and day 30 (31b). A computer-based infrared video system (Med Associates, Inc. USA) was used to monitor the freezing in mice [32].

2.1.7. Tissue processing. Eight representative mice data of each group were used to perform the biochemical analyses. Mice were anesthetized by administering 200μl of ketamine (50 mg/ml, Incepta Pharmaceuticals Ltd., Bangladesh) intraperitoneally. Mice were sacrificed by decapitation. The brain was extracted from the skull and transferred immediately to Petri dishes placed over ice. The hippocampal tissue was microdissected and immediately stored at –80˚C. On the next day, the homogenate of hippocampal tissue 10% (w/v) was prepared in sodium phosphate buffer (1× PBS pH 7.0) supplemented with 1:100 protease inhibitor cocktail (Sigma, Saint Louis, MO, USA) by using Ultra-Turrax T25 (United States) homogenizer. Sonication of homogenized tissue was performed at a 5-s cycle for 150 s using an ultrasonic processor. The homogenized tissue was centrifuged at 10,000 rpm (RCF 11200) for 10 min at 4˚C. The clear supernatants were diluted with 0.1x PBS buffer and performed the biochemical analysis.

2.1.8. Oxidative stress measurement. All determinations were normalized by the protein concentration of the samples. Total protein content was measured by Lowry's method [33].

2.1.8.1. Estimation of Glutathione level. GSH level was detected according to the previous method [34, 35]. Briefly, 2.7 ml of phosphate buffer (0.1 M, pH 8) and 0.2 ml of 5, 5-dithiol-bis (2-nitrobenzoic acid) were added with 1 ml of hippocampal homogenate. The color progressed was determined instantaneously at 412 nm. Results were expressed in μmol/mg protein.

2.1.8.2. Determination of superoxide dismutase activity. The SOD level was estimated based on a modified previous protocol [36, 37]. In short, the reaction mixture carried 50 mM sodium phosphate (pH 7.8), 13 mM methionine, 75 mM nitroblue tetrazolium (NBT), 2 mM riboflavin, 100 mM EDTA and 2 mL of hippocampal tissue homogenate. The change in absorbance of each sample was then documented at 560 nm after forming the blue formazan. The activity of SOD was expressed in U/30sec.

2.1.8.3. Measurement of catalase activity. The CAT activity was measured based on a previous method spectrometrically at a wavelength of 240 nm [38]. The reaction mixture (1.5 ml) comprised 1.0 ml of 0.01 M phosphate buffer (pH 7.0), 0.1 ml of hippocampal tissue homogenate, and 0.4 ml of 2 M H_2O_2. The reaction was stopped by adding 2.0 ml of dichromate-acetic acid reagent (5% potassium dichromate and glacial acetic acid were mixed in a 1:3 ratio). The activity of catalase was expressed in μmol/min/mg protein.

2.1.8.4. Determination of advanced oxidation protein products. AOPP was detected spectrophotometrically using a previous protocol [39, 40]. Briefly, 50 μl of hippocampal tissue homogenate was diluted with phosphate-buffered saline (PBS) at a ratio of 1:2. Chloramine T (0–100

mmol/L) was used for preparing the calibration curve. PBS was used as a blank. 100 μl of 1.16 M potassium iodide and 50 μl of acetic acid were added to each well, and absorbance at 340 nm was determined subsequently. Concentrations of AOPP were represented in chloramine units (μmol/ml).

2.1.8.5. Estimation of nitric oxide level. NO level was estimated according to a previous protocol [41] using the Griess-Illosvoy reagent. Griess–Illosvoy reagent was modified by using naphthyl ethylene diamine dihydrochloride (NED) (0.1% w/v) instead of 1-napthylamine (5%). The hippocampal tissue homogenates, phosphate buffer saline (0.5 mL), NED (1 mL), and sulfanilamide (1 mL) were diluted with PBS (2:8 ratio) and incubated at 25°C for 15 min in a 96-well plate [35]. The absorbances were measured at a wavelength of 540 nm against the blank readings of the spectrophotometer. The concentration of NO was expressed in mmol/mg.

2.1.8.6. Measurement of malondialdehyde level. MDA was detected through colorimetric analysis by determining thiobarbituric acid reactive substances (TBARS) according to a previous protocol [42]. Briefly, 0.1 ml of hippocampal tissue homogenate in Tris–HCl buffer (pH 7.5) was treated with 2 ml of TBA-TCA-HCl (1:1:1 ratio) reagent (thiobarbituric acid 0.37%, 0.25 N HCl, and 15% TCA) and put in a water bath at 70°C for 15 min and cooled. The absorbance of the clear supernatant was estimated against the reference blank at 535 nm [43]. The MDA level was detected by using a standard curve and represented in nmol/ml.

2.2. In silico (molecular docking)

2.2.1. Prediction of molecular target. We predicted the molecular targets of curcumin from the literature search. We also used the SwissTargetPrediction (http://www.swisstarget prediction.ch) webserver [44].

2.2.2. Preparation of protein structures. We downloaded 3D crystallographic structures of target proteins from the Protein Data Bank (https://www.rcsb.org/). Information on the pdb structures is given in Table 1. Protein structures were cleaned in UCSF Chimera [45]. We removed all non-amino acid residues and kept a single chain. The monomeric chain was then subjected to the Dock Prep module of UCSf Chimera, where any incomplete side chains were replaced using the Dunbrack rotamer library. The output from this step was saved as a pdb file. We next converted the pdb file to a pdbqt file using AutoDockTools [46]. Polar hydrogen atoms were added during this step, nonpolar hydrogens were merged, and the Kollman charges were added.

2.2.3. Preparation of ligand structures. Curcumin's (PubChem CID: 969516) canonical slimes and 2D structure (as sdf) were obtained from PubChem (https://pubchem.ncbi.nlm.nih. gov/). We checked the accompanying literature for protein crystal structures, and Co-crystallized reference ligands were saved as pdb files in UCSF Chimera. All ligand structures were processed and saved as pdbqt files using Open babel [47] and POAP [48]. In short, ligands were optimized using the MMFF94 force field, all hydrogen atoms were added, 3D structures were generated, and energy minimization was done using 5000 steps of the conjugate algorithm.

Table 1. Information of protein structures.

Protein Name	Common Name	UniProt ID	PDB ID	Reference Ligand (Co-crystallized)	Reference
Beta-secretase 1	BACE1	P56817	2QP8	SCH734723	[86]
Glutathione S-transferase A1	GSTA1	P08263	4HJ2	Chlorambucil	[87]
Glutathione S-transferase omega-1	GSTO1	P78417	4YQM	C1-27	[88]
Kelch-like ECH-associated protein 1	KEAP1	Q14145	6TYM	08A	[89]
Amine oxidase [flavin-containing] A	MAOA	P21397	2Z5X	Harmine	[90]

https://doi.org/10.1371/journal.pone.0270123.t001

2.2.4. AutoDock Vina molecular docking. We performed Vina molecular docking [46] using the virtual screening tool of POAP. The grid box size was 24x24x24 angstroms, and the box was centered on the co-crystallized ligand in the pdb structure. The exhaustiveness was 8 for Vina docking. We recorded the estimated binding energy values for the best-docked poses of the ligands.

2.2.4.1. Protein-ligand interactions. From Vina docking simulations, we retrieved pdb files of the complexes with the best-docked poses (lowest estimated binding energy). Protein-ligand interactions were visualized using Discovery Studio Visualizer (BIOVIA, Dassault Systèmes, Discovery Studio Visualizer, v20.1.0.192, 2019). We compared the interactions of the co-crystallized ligand in the pdb file with that of the curcumin.

2.2.4.2. 3D-rendering of protein-ligand complexes. We used open-source Pymol [49] to render 3D images of ligands and the binding sites in the proteins.

2.3. Statistical analysis

A One-Way ANOVA followed by the Brown-Forsythe test was performed to determine the effect of the treatment groups. All analyses were executed by the GraphPad prism software. The difference was considered significant when the p-value was less than 0.05. Data were represented as mean ± SEM (Standard Error of the Mean).

2.4. Ethics

The institutional animal care and use committee (IACUC) of North South University (2019/ OR-NSU/IACUC- No.0903) approved the study protocol. All the experimental procedures were performed following the NIH Guide for the care and use of laboratory animals. Throughout the experiments, all efforts were given to minimize the number of animals and to optimize their comfort.

3. Results

3.1. Effects of curcumin on retention time by adopting passive avoidance task

After 24 hours of training, the Vehicle and Curcumin-Control (Cur-Con) groups displayed mean retention times (RTs) of 210.93 ± 6.33 s and 276.31 ± 8.51 s, respectively (Fig 2). The RT was 116.43 ± 2.62 s in the D-gal injected mice group, indicating a significant decrease compared with the Vehicle ($F_{1, 14} = 2.07$, $p < 0.0001$) and the Cur-Con ($F_{1, 14} = 2.17$, $p < 0.0001$) groups (Fig 2). Contrarily, the decreasing trend of RT was prominently protected in the Curcumin + D-gal mice group (255.62 ± 14.11 s) (Fig 2). A One-Way ANOVA followed by the Brown-Forsythe test demonstrated a statistically significant difference in RT values between the Curcumin + D-gal and the D-gal injected mice groups ($F_{1, 14} = 88.31$, $p < 0.0001$). An RT value of 249.87 ± 8.97 s was observed in the Ast + D-gal mice, which was significantly higher than the D-gal treated mice group ($F_{1, 14} = 7.95$, $p > 0.05$; Fig 2). A similar tendency was observed in NA mice. The RT was 132.12 ± 3.11 s in the NA mice group (Fig 2). On the contrary, compared to the NA mice group, there was a significant protection from the decreasing trend of RT observed in the Curcumin + NA (247.25 ± 10 s; $F_{1, 14} = 31.10$, $p < 0.0001$) and Ast + NA (269.81 ± 8.02 s; $F_{1, 14} = 2.06$, $p < 0.0001$) mice groups (Fig 2).

Similarly, after 48 hours of training, the Vehicle and Cur-Con groups exhibited RTs of 202.43 ± 3.99 s, 271.87 ± 5.41 s, respectively (S1 Fig). As expected, RT values were considerably low in the D-gal injected mice (105.87 ± 3.58 s) and significantly high both in the Curcumin + D-gal (246.81 ± 14.38 s) and the Ast + D-gal mice (239.75 ± 10.04 s) (S1 Fig). Comparables
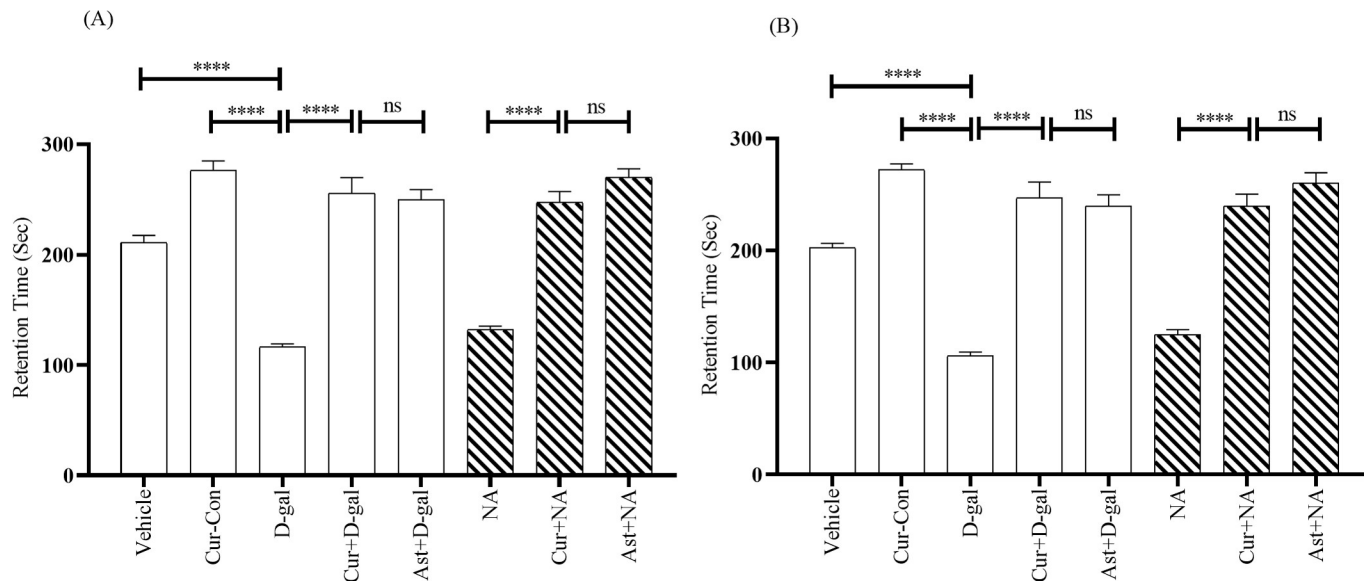
Fig 2. Effect of curcumin on RT in D-gal and NA mice group after 24 hours of training. The RT was calculated by performing PA tasks among Vehicle, Cur-Con, D-gal, Curcumin + D-gal, Ast + D-gal, NA, Curcumin + NA, Ast + NA groups. RT was expressed in second. Data was presented as mean ± SEM, n = 8 each group; ****p < 0.0001, ns = not significant.

RTs were also observed in the NA (125.06 ± 4.33 s), the Curcumin + NA (239.81 ± 10.38 s), and the Ast + NA (260.31 ± 9.16 s) groups.

3.2. Effects of curcumin on freezing response by performing contextual fear conditioning task

3.2.1. Effects of curcumin on freezing response in conditioning session. The contextual fear conditioning test was performed to evaluate the fear memory. On day 2(2a) of conditioning, the baseline activity was evaluated during the first 2 minutes in the novel environment. In this session, freezing response (FR) was detected without presenting the conditioned stimulus (CS, white noise) or unconditioned stimulus (US, foot-shock). The baseline activity was almost similar among Vehicle, Cur-Con, D-gal, Curcumin + D-gal, and Ast + D-gal groups (Fig 3A). During the last 6 min with CS-US pairings, the Vehicle and Cur-Con groups exhibited an FR of 61.87 ± 3.45%, 71.45 ± 3.17%, respectively (Fig 3A). The D-gal administered mice displayed an FR, 42.5 ± 3.60%, indicating a significant decrease compared with the Vehicle ($F_{1, 14} = 0.39$, p < 0.001) and the Cur-Con ($F_{1, 14} = 0.52$, p < 0.0001) groups (Fig 3A). Intriguingly, the decreasing tendency of FR was significantly protected in the Curcumin + D-gal mice group (67.60 ± 2.62%; $F_{1, 14} = 0.76$, p < 0.0001; Fig 3A) and similar trend was detected in the Ast (standard antioxidant drug) +D-gal mice group (66.56 ± 1.77%; $F_{1, 14} = 1.96$, p > 0.05). Likewise, the baseline activity was almost similar among the NA, Curcumin + NA, and Ast + NA groups (Fig 3B). During the last 6 minutes with CS-US pairing, the NA group exhibited an FR of 45.62 ± 0.82% (Fig 3B). Contrarily, compared to the NA mice group, the declining trend of FR was remarkably protected in the Curcumin + NA (64.79 ± 2%; $F_{1, 14} = 10.41$, p < 0.0001) mice group (Fig 3B). A similar change in FR was observed in the Ast (standard antioxidant drug) +NA mice group (63.95 ± 2.88%; p > 0.05; Fig 3B).

On day 31(31a) of conditioning, the Vehicle and Cur-Con groups displayed an FR of 55.83 ± 3.53%, and 66.04 ± 2.51%, respectively, during the last 6 min with CS-US pairings (Fig 3A). The FR was 35 ± 2.45% in the D-gal administered mice group, illustrating a significant
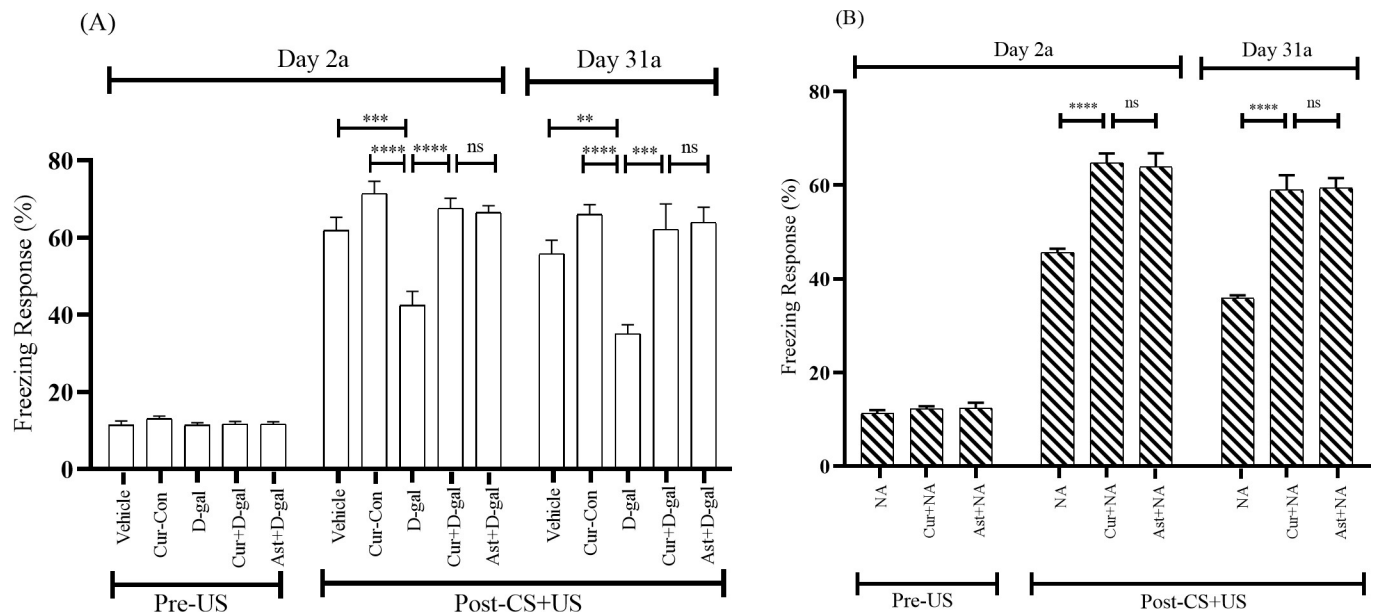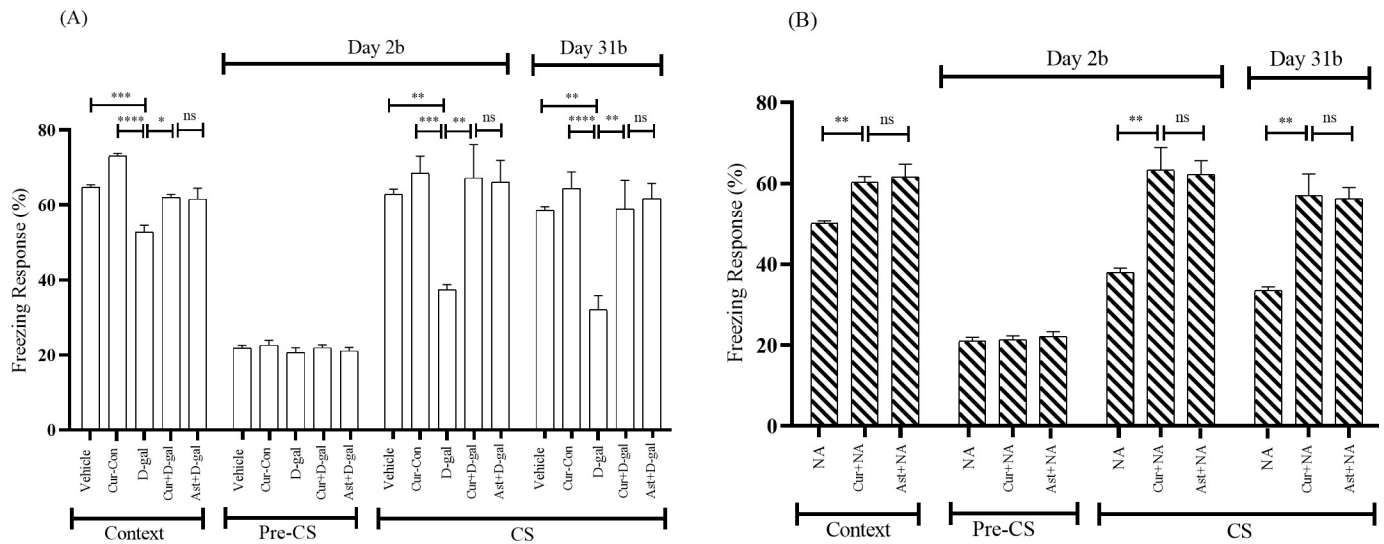
Fig 3. Effect of curcumin on the conditioning fear memory of (A) D-gal and (B) NA mice group. The memory was assessed by analyzing the FR. The FR was expressed in percentage (%). Data was presented as mean ± SEM, n = 8 each group; **p < 0.01, ***p < 0.001, ****p < 0.0001, ns = not significant.

https://doi.org/10.1371/journal.pone.0270123.g003

decrease compared with the Vehicle ($F_{1, 14}$ = 2.48, p < 0.01) and the Cur-Con ($F_{1, 14}$ = 0.01, p < 0.0001) groups (Fig 3A). As expected, compared to the D-gal treated mice group, a significant protection from the decreasing tendency of FR was detected in the Curcumin + D-gal (62.18 ± 6.57%; $F_{1, 14}$ = 5.44, p < 0.001) mice group (Fig 3A). This FR was comparable to the FR exhibited by the Ast (standard antioxidant) + D-gal mice (63.95 ± 3.95%; $F_{1, 14}$ = 2.54, p > 0.05; Fig 3A). A similar pattern was observed in the NA group. During the last 6 min with CS-US pairings, the NA group displayed an FR of 35.83 ± 0.62% (Fig 3B). A significant protection from the decreasing tendency of FR was found in Curcumin + NA (58.95 ± 3.16%; $F_{1, 14}$ = 6.89, p < 0.0001; Fig 3B) group mice (Fig 3B). An equivalent FR elevation was also apparent in the Ast (standard antioxidant drug) + NA group (59.37 ± 2.13%; $F_{1, 14}$ = 1.16, p > 0.05; Fig 3B).

3.2.2. Effects of curcumin on freezing response in context test. During the last 6 min with CS-US pairings, the Vehicle and Cur-Con groups exhibited FR of 64.72 ± 0.70% and 73.05 ± 0.74%, respectively. The FR was 52.77 ± 1.85% in the D-gal treated mice group, indicating a significant decrease compared with the Vehicle ($F_{1, 14}$ = 4.83, p < 0.001) and Cur-Con ($F_{1, 14}$ = 4.63, p < 0.0001) groups (Fig 4A). On the contrary, a significant protection from the the declining trend of FR was detected in the Curcumin + D-gal (62.01 ± 0.83%; $F_{1, 14}$ = 3.38, p < 0.05) and was comparable to the FR exhibited by the Ast (standard antioxidant drug) + D-gal treated mice group (61.59 ± 2.88%; $F_{1, 14}$ = 9.30, p > 0.05; Fig 4A). During the last 6 min with CS-US pairings, the NA group displayed an FR of 50.13 ± 0.57% (Fig 4B). This decreasing tendency of FR was remarkably prevented in the Curcumin + NA mice group (60.27 ± 1.38%; $F_{1, 14}$ = 9.72, p < 0.01; Fig 4B). This FR was comparable to the FR exhibited by the standard drug (Ast) in Ast + NA (62.36 ± 3.16%; $F_{1, 14}$ = 7.81, p > 0.05; Fig 4B) mice group.

3.2.3. Effects of curcumin on freezing response in cued test. In the cued test following the context test, mice were placed in a differently shaped chamber with altered context. During the first 3 min period with Pre-CS presentation, the baseline activity was almost similar among Vehicle, Cur-Con, D-gal, Curcumin + D-gal, and Ast (standard antioxidant) + D-gal groups (Fig 4A). On day 2(2b), during the last 3 min of the cued test with CS presentation, the Vehicle

(A)

(B)

Fig 4. Effect of curcumin on the context and cued fear memory (Day 2b and 31b) of (A) D-gal and (B) NA mice group. The memory was assessed by analyzing the FR. The FR was expressed in percentage (%). Data was presented as mean ± SEM, n = 8 each group; *p < 0.05, **p < 0.01, ***p < 0.001, ****p < 0.0001, ns = not significant.

and Cur-Con groups exhibited an FR of 62.84 ± 1.37% and 68.43 ± 4.58%, respectively (Fig 4A). The percentage of FR was considerably low in the D-gal administered mice (37.43 ± 1.36%), significantly high both in the Vehicle ($F_{1, 14}$ = 0.30, p < 0.01) and and Cur-Con ($F_{1, 14}$ = 4.62, p < 0.001). Compared to the decreasing tendency of the percentage of FR displayed by the D-gal treated mice group, there was significant protection detected in the Curcumin + D-gal (67.23 ± 8.87%) and Ast + D-gal mice groups (66.11 ± 5.82%) (Fig 4A). The differences in FR were remarkable between D-gal and Curcumin + D-gal groups ($F_{1, 14}$ = 26.64, p < 0.01) but indistinguishable between Curcumin + D-gal and standard drug (Ast) + D-gal groups ($F_{1, 14}$ = 3.15, p > 0.05; Fig 4A). The baseline activity did not differ among the NA, Curcumin + NA, and Ast + NA groups (Fig 4B). On day 2(2b), during the last 3 min of the cued test with CS presentation, the NA group displayed an FR of 38.05 ± 1.03% (Fig 4B). On the contrary, the declining tendency of FR was prevented in the Curcumin + NA mice group (63.28 ± 5.58%; Fig 4B). One-Way ANOVA revealed that the FR elevation in Curcumin + NA mice was statistically significant ($F_{1, 14}$ = 13.69, p < 0.01) compared to the NA mice and comparable to that in the standard antioxidant group (Ast + NA) mice group (62.22 ± 3.39%; $F_{1, 14}$ = 2.51, p > 0.05; Fig 4B).

On day 31(31b), during the last 3 min of the cued test with CS presentation, The percentage of FR was 32.15 ± 3.73 in the D-gal injected mice group, indicating a significant decrease compared with the Vehicle (58.54 ± 0.98%; $F_{1, 14}$ = 7.94, p < 0.01) and the Cur-Con (64.47 ± 4.36%; $F_{1, 14}$ = 0.34, p < 0.0001) groups (Fig 4A). Compared to the declining trend of the percentage of FR displayed by the D-gal treated mice group, significant protection was seen in Curcumin + D-gal treated mice group (58.98 ± 7.58%; $F_{1, 14}$ = 6.09, p < 0.01; Fig 4A). This percentage of FR was similar to the FR exhibited by the standard drug (Ast) + D-gal-treated mice (61.66 ± 4.09%; $F_{1, 14}$ = 4.89, p > 0.05; Fig 4A). A similar trend was observed in the NA group. During the last 3 min of the cued test with CS presentation, the NA group exhibited an FR of 33.47 ± 0.90% (Fig 4B). Contrarily, this change of FR was remarkably protected in the Curcumin + NA mice group (57.03 ± 5.29%; $F_{1, 14}$ = 8.47, p < 0.01; Fig 4B). This FR was comparable to the FR exhibited by the Ast + NA group (56.18 ± 2.81%; $F_{1, 14}$ = 2.34, p > 0.05; Fig 4B).

### 3.3. Effects of curcumin on oxidative stress biomarkers

3.3.1. Glutathione. The GSH level detected in the Vehicle and Cur-Con groups were 9.34 ± 0.87 μmol/mg and 12.72 ± 0.97 μmol/mg, respectively (Fig 5A). The level of GSH in the D-gal treated mice group was 3.19 ± 0.31 μmol/mg, illustrating a significant decrease of GSH compared with Vehicle ($F_{1, 14}$ = 3.63, $p < 0.0001$) and Cur-Con ($F_{1, 14}$ = 2.58, $p < 0.0001$) groups (Fig 5A). The GSH level in Curcumin + D-gal mice group was 10.77 ± 1.02 μmol/mg, indicating a remarkable protection from the decreasing trend of GSH level ($F_{1, 14}$ = 16.49, $p < 0.0001$) (Fig 5A). A similar GSH elevation was apparent in the Ast + D-gal mice (10.81 ± 0.52 μmol/mg; $F_{1, 14}$ = 7.73, $p > 0.05$; Fig 5A).

The GSH level in the NA group was 3.78 ± 0.59 μmol/mg (Fig 5B). Conversely, this decreasing trend of GSH level was remarkably prevented in the Curcumin + NA mice group (10.16 ± 0.74 μmol/mg; $F_{1, 14}$ = 0.46, $p < 0.0001$; Fig 5B). This GSH level was comparable to the GSH level detected in the Ast + NA (11.28 ± 0.61 μmol/mg; $F_{1, 14}$ = 0.74, $P > 0.05$; Fig 5B) mice group.

3.3.2. Superoxide dismutase. The SOD activity was 27.16 ± 0.32 U/30s and 40.24 ± 3.46 U/30s in the Vehicle and Cur-Con groups, respectively (Fig 5C). The SOD activity in D-gal administered mice group was 11.45 ± 0.27 U/30s, indicating a significant decrease in the activity compared with Vehicle ($F_{1, 14}$ = 0.25, $p < 0.05$) and Cur-Con ($F_{1, 14}$ = 21.52, $p < 0.0001$) groups (Fig 5C). Interestingly, curcumin produced an efficient protection of the SOD activity (35.68 ± 3.46 U/30s) detected in Curcumin + D-gal mice group, which was statistically significant ($F_{1, 14}$ = 28.37, $p < 0.0001$) compared to the D-gal treated mice group but insignificant compared to the Ast + D-gal group (37.27 ± 5.46 U/30s; $F_{1, 14}$ = 0.67, $p > 0.05$; Fig 5C) mice.

The SOD activity in the NA mice group was 13.03 ± 0.26 U/30s (Fig 5D). Contrarily, this decreasing activity was protected in the Curcumin + NA mice group (31.27 ± 1.63 U/30s; Fig 5D). A One-Way ANOVA followed by the Brown-Forsythe test demonstrated a statistically significant change in the SOD activity of the curcumin mice compared to the SOD activity of the NA mice ($F_{1, 14}$ = 7.15, $p < 0.01$). The effect of curcumin on the SOD activity was very similar to the effect of Ast (35.39 ± 4.80 U/30s; $F_{1, 14}$ = 14.68, $p > 0.05$; Fig 5D) found in Ast + NA group mice.

3.3.3. Catalase. The CAT activity was 6.83 ± 0.39 μmol/min/mg and 12.33 ± 0.92 μmol/min/mg in the Vehicle and Cur-Con groups, respectively. The CAT activity in D-gal treated mice group was 2.82 ± 0.18 μmol/min/mg, illustrating a significant decrease in activity
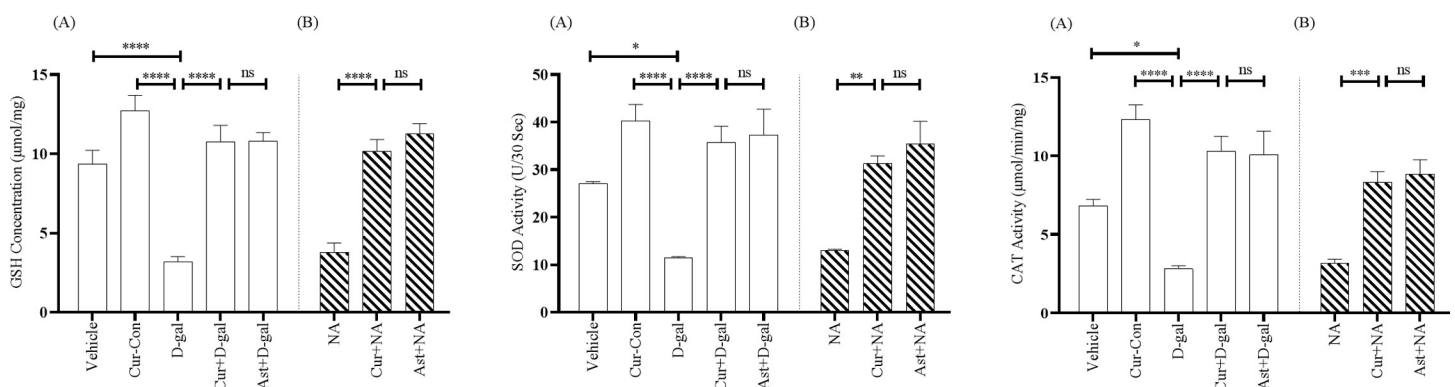
Fig 5. Effect of curcumin on GSH concentration (A and B), SOD (C and D) and CAT (E and F) activity in D-gal and NA mice group. The GSH, SOD, CAT was detected by using bioassay technique among Vehicle, Cur-Con, D-gal, Curcumin + D-gal, Ast + D-gal, NA, Curcumin + NA, Ast + NA groups. GSH level, SOD and CAT activity were expressed in μmol/mg, U/30s, and μmol/min/mg, respectively. Data was presented as mean ± SEM, n = 8 each group; *p < 0.05, **p < 0.01 ***p < 0.001, ****p < 0.0001 ns = not significant.

https://doi.org/10.1371/journal.pone.0270123.g005

compared with Vehicle ($F_{1, 14} = 0.81$, $p < 0.05$) and Cur-Con ($F_{1, 14} = 29.53$, $p < 0.0001$) groups (Fig 5E). On the contrary, a statistical significant protection from the decreasing activity of CAT activity was detected in the Curcumin + D-gal mice group (10.29 ± 0.95 μmol/min/mg; $F_{1, 14} = 4.6$, $p < 0.0001$; Fig 5E). This activity was comparable to the CAT activity of Ast + D-gal mice group (10.06 ± 1.51 μmol/min/mg; $F_{1, 14} = 0.78$, $p > 0.05$; Fig 5E).

Similarly, the CAT activity in the NA mice was 3.15 ± 0.26 μmol/min/mg (Fig 5F). Curcumin produced efficient protection of the CAT activity (8.31 ± 0.22 μmol/min/mg Fig 5F), detected in the Curcumin + NA mice group. A One-Way ANOVA followed by the Brown-Forsythe test confirmed a statistically significant change in the CAT activity by curcumin ($F_{1, 14} = 0.47$, $p < 0.001$) compared to the CAT activity of the NA mice. This CAT activity was comparable to that of the Ast + NA mice (8.85 ± 0.91 μmol/min/mg; $F_{1, 14} = 3.24$, $p > 0.05$; Fig 5F).

3.3.4. Advanced oxidation of protein products. The AOPP level was drastically elevated to 146.41 ± 16.60 μmol/ml in the D-gal group, illustrating a significant increase of AOPP level compared with the Vehicle (84.80 ± 11.87 μmol/ml; $F_{1, 14} = 0.99$, $p < 0.01$) and Cur-Con (49.65 ± 7.03 μmol/ml; $F_{1, 14} = 5.11$, $p < 0.0001$) groups (Fig 6A). However, a statistical significant protection from the increasing tendency of AOPP level was found in the Curcumin + D-gal mice group (61.55 ± 10.80 μmol/ml; Fig 6A; $F_{1, 14} = 2.30$, $p < 0.0001$), but was indistinguishable from the Ast + D-gal group (56.44 ± 10.44 μmol/ml; $F_{1, 14} = 0.13$, $p > 0.05$; Fig 6A). Similarly, the AOPP level was significantly declined to 69.52 ± 9.90 μmol/ml in the Curcumin + NA mice group compared to the NA (137.67 ± 15.24 μmol/ml) mice ($F_{1, 14} = 0.76$, $p < 0.01$; Fig 6B) group. This level was comparable to the level of Ast + NA mice group (61.28 ± 7.04 μmol/ml; $F_{1, 14} = 0.28$, $p > 0.05$; Fig 6B).

3.3.5. Nitric oxide. D-gal administration profoundly enhanced the NO level to 9.40 ± 1.01 mmol/mg, indicating a significant increase of NO level compared with the Vehicle (4.62 ± 0.33 mmol/mg; $F_{1, 14} = 6.02$, $p < 0.0001$) and Cur-Con (3.23 ± 0.75 mmol/mg; $F_{1, 14} = 0.22$, $p < 0.0001$) groups (Fig 6C). Conversely, a statistical significant protection from the increasing tendency of NO level was detected in the Curcumin + D-gal mice group (4.47 ± 0.53 mmol/mg; $F_{1, 14} = 2.75$, $p < 0.0001$; Fig 6C). This level was comparable to the NO level of Ast + D-gal mice (4.09 ± 0.55 mmol/mg; $F_{1, 14} = 0.32$, $p > 0.05$; Fig 6C). A similar pattern was observed in the normal-aged mice. The NO level in the NA group was 8.06 ± 0.29 mmol/mg (Fig 6D). On the contrary, this increasing tendency of NO level was prevented in the Curcumin + NA (5.28 ± 0.25 mmol/mg) group mice (Fig 6D). A One-Way ANOVA followed by the Brown-Forsythe test demonstrated a statistically significant effect of curcumin
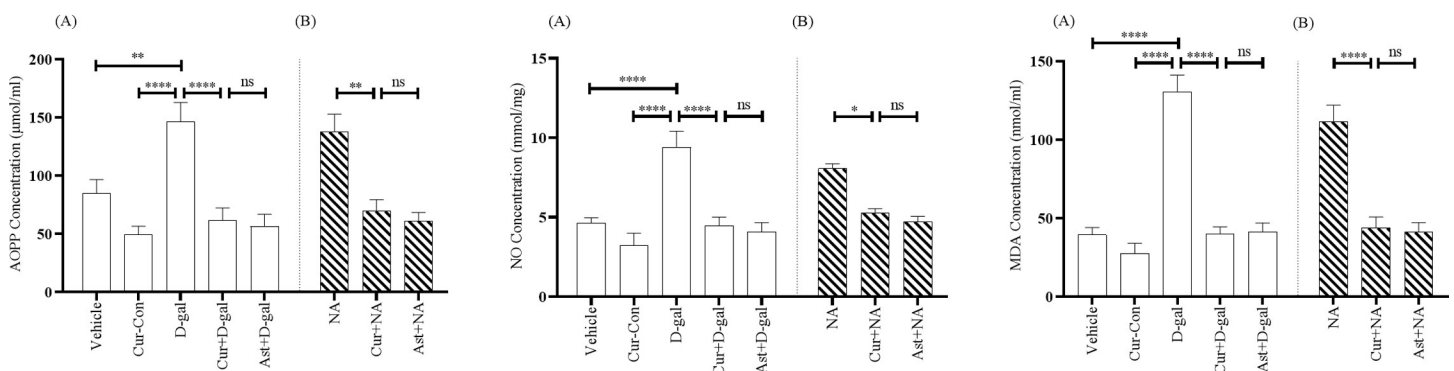
Fig 6. Effect of curcumin on AOPP (A and B), NO (C and D), and MDA (E and F) concentration in D-gal and NA mice group. The AOPP level was assessed using bioassay technique among Vehicle, Cur-Con, D-gal, Curcumin + D-gal, Ast + D-gal, NA, Curcumin + NA, Ast + NA groups. AOPP, NO, and MDA level was represented in μmol/ml, mmol/mg, and nmol/ml, respectively. Data was presented as mean ± SEM, n = 8 each group; *$p < 0.05$, **$p < 0.01$, ****$p < 0.0001$ ns = not significant.

Table 2. Estimated binding energies from Vina molecular docking.

| Protein	PDB ID	Reference Ligand	Binding Energy (kcal/mol)	
			Curcumin	Reference Ligand
BACE1	2QP8	SCH734723	-8.5	10
GSTA1	4HJ2	Chlorambucil	-9.6	-7.5
GSTO1	4YQM	C1-27	-8.6	-6.6
KEAP1	6TYM	08A	-8.6	-9.2
MAOA	2Z5X	Harmine	-9.2	-8.7

($F_{1, 14}$ = 0.91, p < 0.05). The NO level in the curcumin mice was comparable to that of the Ast + NA mice group (4.72 ± 0.33 mmol/mg; $F_{1, 14}$ = 1.64, p > 0.05; Fig 6D).

3.3.6. Lipid peroxidation. The MDA level was 39.37 ± 4.62 nmol/ml and 27.64 ± 6.40 nmol/ml in the Vehicle and Cur-Con groups, respectively. The level of MDA in the D-gal group was 130.37 ± 10.81 nmol/ml, indicating a significant increase in the MDA level compared with Vehicle ($F_{1, 14}$ = 5.32, p < 0.0001) and Cur-Con ($F_{1, 14}$ = 2.69, p < 0.0001) groups (Fig 6E). A statistical significant protection from the increasing trend of MDA level was found in the Curcumin + D-gal mice group (40.05 ± 4.39 nmol/ml; $F_{1, 14}$ = 5.66, p < 0.0001; Fig 6E). This MDA level was comparable to that of the Ast + D-gal mice group (41.29 ± 5.53 nmol/ml; $F_{1, 14}$ = 0.78, p > 0.05; Fig 6E). Similarly, the MDA level in the NA group was 111.50 ± 10.49 nmol/ml (Fig 6F). Interestingly, this increasing pattern of the MDA level was significantly prevented in the Curcumin + NA mice group (43.74 ± 6.97 nmol/ml; $F_{1, 14}$ = 0.53, p < 0.0001) and was comparable to the Ast + NA mice group (41.08 ± 6.06 nmol/ml; ($F_{1, 14}$ = 0.31, p > 0.05; Fig 6F).

3.4. Molecular docking

Curcumin significantly attenuated oxidative stress in our in vivo aging model. We performed molecular docking to predict interactions of curcumin with glutathione S-transferase A1 (GSTA1), glutathione S-transferase omega-1(GSTO1), and kelch-like ECH-associated protein 1(KEAP1), which play significant roles in redox signaling to regulate cellular events such as senescence. GSTA1 and GSTO1, which belong to the ROS/RNS neutralizing enzyme gene family glutathione transferase (GST), catalyze GSH conjugation with reactive electrophiles and detoxify hydroperoxides for maintaining redox homeostasis [50]. KEAP1, a central key sensor that regulates the expression of many cytoprotective genes in oxidative and electrophile stress, targets nuclear factor-erythroid 2-related factor 2 (Nrf2) in modulating redox homeostasis [51]. We first performed Vina molecular docking simulations of curcumin using 3D crystallographic structures of GSTA1, GSTO1, and KEAP1. Estimated binding energy values (kcal/mol) are given in Table 2. In general, a more negative value is an indication of a more stable complex. When docked to GSTA1, curcumin had lower binding energy than the co-crystallized ligand chlorambucil (-9.6 vs. -7.5) (Table 2). Analysis of docking poses revealed that the chlorambucil was redocked at the same binding pocket with a slightly different binding pose than observed in the pdb file (Fig 7A). The predicted binding site of curcumin matched that of redocked chlorambucil (Fig 7B). In the GSTA1 crystal structure, chlorambucil forms a salt bridge, three hydrogen bonds, and multiple van der Waals interactions (Fig 7C). On the other hand, curcumin is predicted to form a pi-sigma bond with ALA100 and multiple van der Waals interactions (Fig 7D). Both curcumin and chlorambucil can interact with the residues GLY14, THR68, ILE106, LEU107, and MET208 of GSTA1 through van der Waals interactions. Overall, curcumin is predicted to bind GSTA1 with favorable interactions. Compared to the
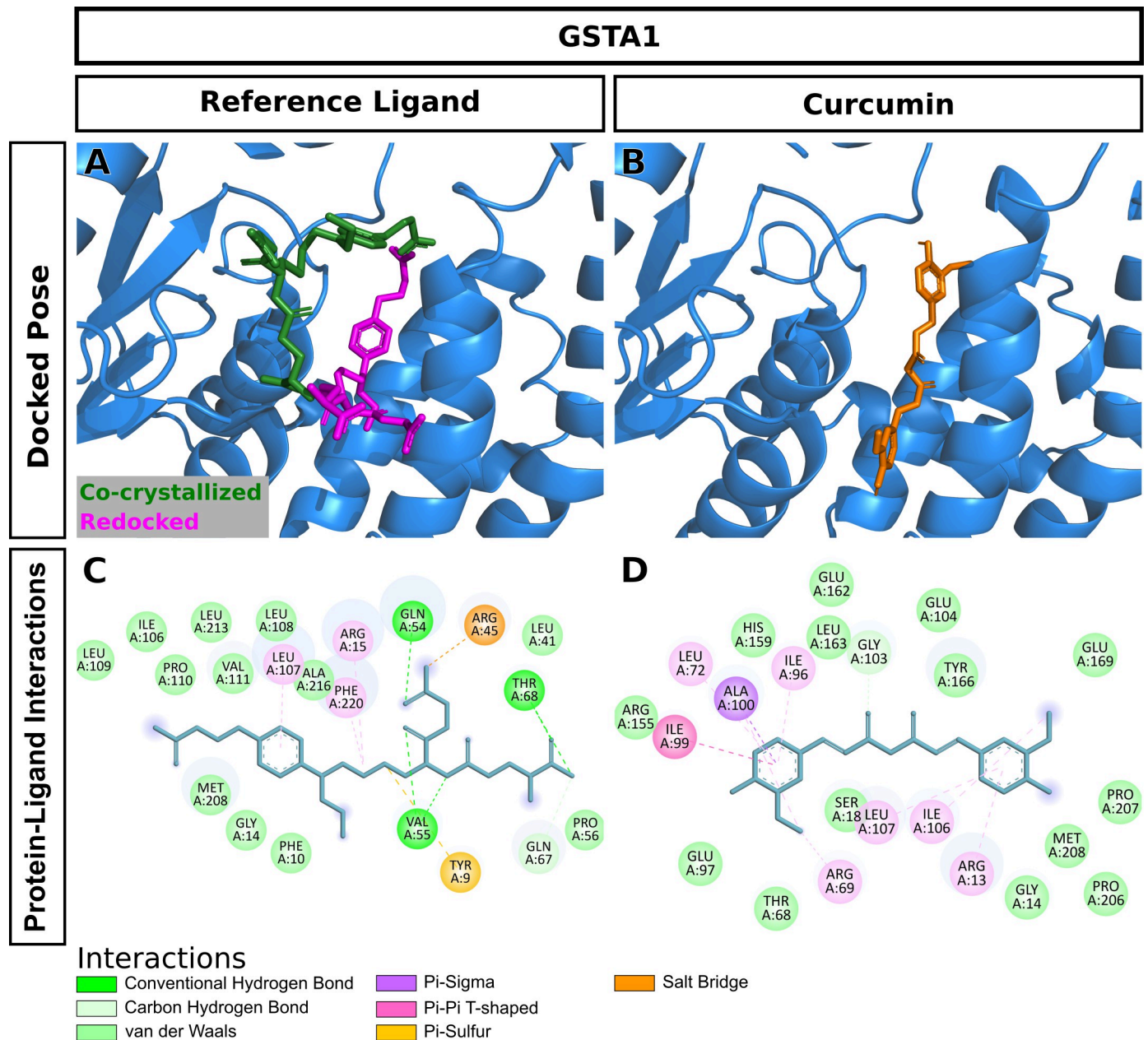
Fig 7. Molecular docking of curcumin to GSTA1. (A) Redocking of the bound ligand. (B) Docking pose of curcumin. (C) Interactions of the bound ligand with the protein. (D) Predicted interactions of curcumin with the protein.

reference ligand C1-27, curcumin also had a stronger binding affinity for GSTO1 (Table 2). Vina performed exceptionally well to reproduce the docking pose of the co-crystallized inhibitor C1-27 (Fig 8A). Interestingly, curcumin also occupied the binding pocket of GSTO1 (Fig 8B) with an extended structure. More importantly, many interacting residues, including CYS32, PRO33, PHE34, LEU56, VAL72, PRO124, ILE131, TRP180, and TYR229, were common for curcumin and C1-27 (Fig 8C and 8D). It can be assumed that curcumin will be a potent inhibitor for GSTO1. For KEAP1, Vina docking showed a slightly weaker interaction of curcumin than the bound ligand (Table 2). Both curcumin and the reference ligand 08A were
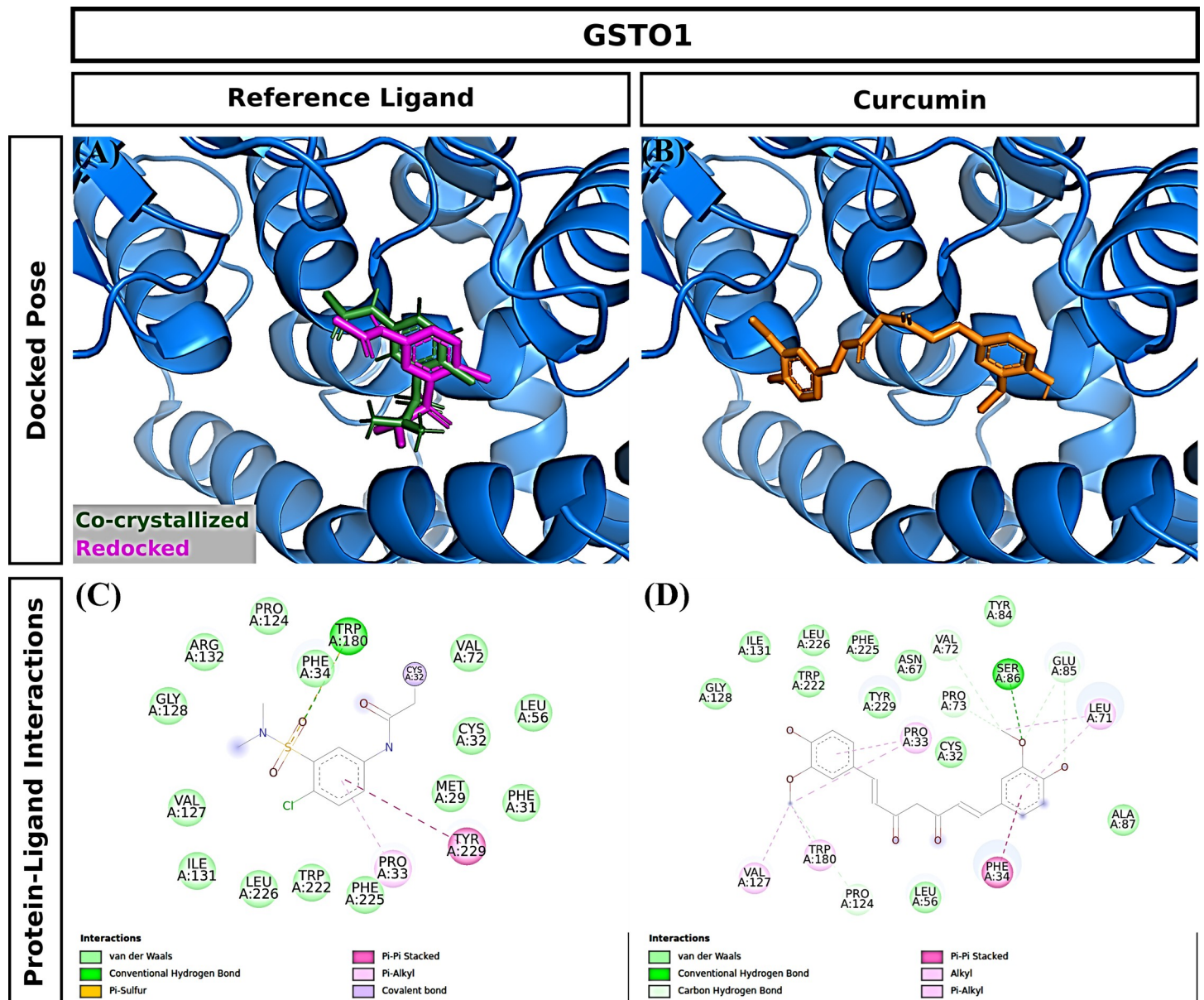
Fig 8. Molecular docking of curcumin to GSTO1. (A) Redocking of the bound ligand. (B) Docking pose of curcumin. (C) Interactions of the bound ligand with the protein. (D) Predicted interactions of curcumin with the protein.

docked at the binding pocket of KEAP1 with a different pose than that of the bound ligand in the crystal structure (Fig 9A and 9B). Many residues interacting with 08A were also predicted to form van der Waals interactions with curcumin (Fig 9C and 9D). Curcumin forms at least two hydrogen bonds and one Pi-Sigma bond with KEAP1 (Fig 9D). Thus, curcumin is predicted as a ligand for KEAP1. To explore additional molecular targets of Cur, we used the SwissTargetPrediction (http://www.swisstargetprediction.ch) webserver. Among the top 50 targets, 26% (15/50) were kinases, 16% lyases (8/50), 10% (5/50) proteases, and 6% (3/50) oxidoreductases (Fig 10). The top ten predicted target proteins are shown in Fig 11. The predicted targets also included five proteins, including the oxidoreductase MAOA, with a probability of 1 (on a scale of 0–1), for which curcumin is a known active. Next to these perfect hits, BACE1 yielded
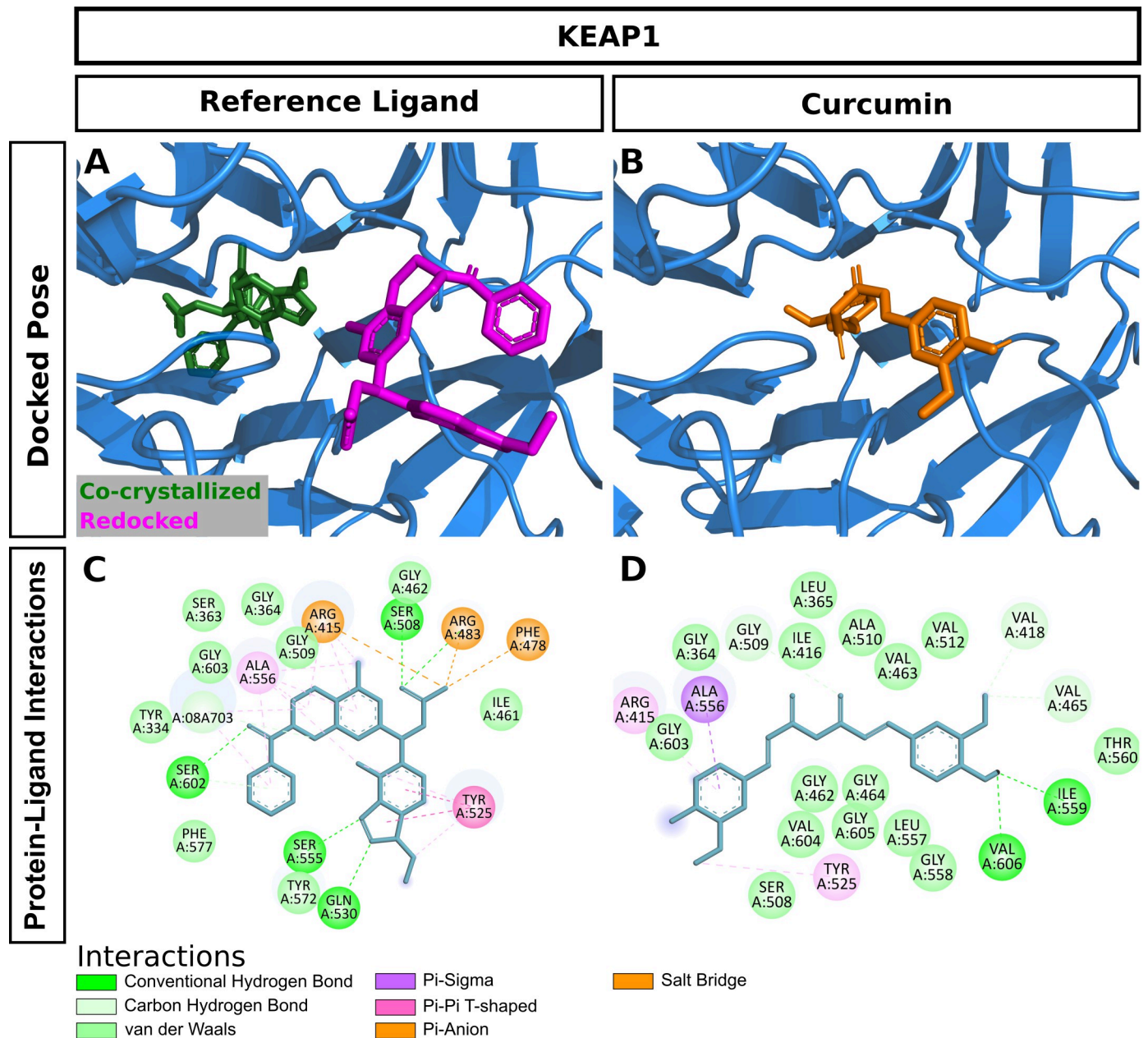
Fig 9. Molecular docking of curcumin to KEAP1. (A) Redocking of the bound ligand. (B) Docking pose of curcumin. (C) Interactions of the bound ligand with the protein. (D) Predicted interactions of curcumin with the protein.

a very high probability score (0.83) (Fig 11). Vina docking showed a higher binding affinity (Table 2) and comparable binding interactions of curcumin (Fig 12B and 12D) and the bound ligand harmine (Fig 12A and 12C) for MAOA, supporting the SwissTargetPrediction results. For BACE1, the estimated binding energies were -8.5 and -10 for curcumin and SCH734723, respectively (Table 2). In this case, Vina redocking perfectly matched the docking pose of SCH734723 in the BACE1 crystal structure (Fig 13A). Curcumin was also predicted to dock at the same binding pocket (Fig 13B). Intriguingly, multiple similar amino acid residues of BACE1 are likely to interact with both the reference ligand and curcumin (Fig 13C and 13D).
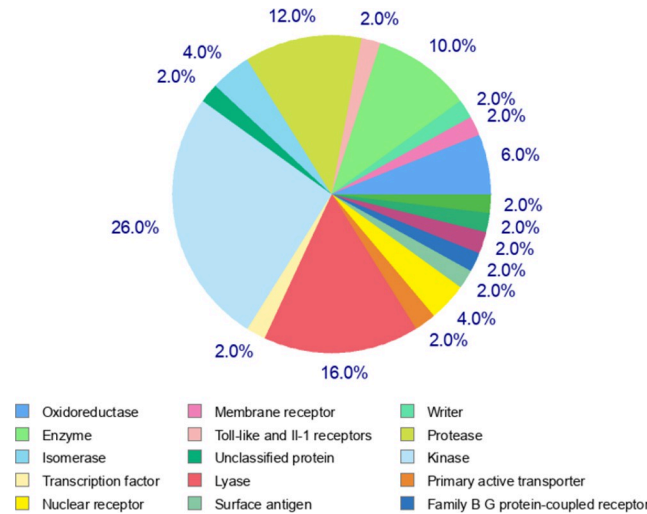
Fig 10. Relative abundance of the class of top 50 predicted molecular targets of curcumin obtained from SwissTargetPrediction.

https://doi.org/10.1371/journal.pone.0270123.g010

For instance, GLY72, GLN73, ILE171, and TYR132 interact with both molecules. Ser71, GLY74, and ARG296 can form conventional hydrogen bonds with the curcumin. Overall, our molecular docking identifies curcumin as a candidate BACE1 inhibitor.

4. Discussion

This current study investigated the effects of curcumin on D-gal and normal aging-induced memory impairment. In vivo study revealed that curcumin protected the decreasing tendency of D-gal and Normal aging-induced RT and FR in PA and CFC tasks. In addition, curcumin ameliorated the level of oxidative stress biomarkers (GSH, SOD, CAT, AOPP, NO MDA). In silico study discerned that curcumin-mediated antioxidant effects in mice could result from, at least partially, binding with several regulatory proteins such as GSTA1, GSTO1, KEAP1, BACE1, and MAOA.

Target	Common name	Uniprot ID	ChEMBL ID	Target Class	Probability*
Monoamine oxidase A	MAOA	P21397	CHEMBL1951	Oxidoreductase	
Beta amyloid A4 protein	APP	P05067	CHEMBL2487	Membrane receptor	
Histone acetyltransferase p300	EP300	Q09472	CHEMBL3784	Writer	
Prostaglandin E synthase	PTGES	O14684	CHEMBL5658	Enzyme	
Toll-like receptor (TLR7/TLR9)	TLR9	Q9NR96	CHEMBL5804	Toll-like and Il-1 receptors	
Beta-secretase 1	BACE1	P56817	CHEMBL4822	Protease	
DNA topoisomerase II alpha	TOP2A	P11388	CHEMBL1806	Isomerase	
Nuclear factor erythroid 2-related factor 2	NFE2L2	Q16236	CHEMBL1075094	Unclassified protein	
Arachidonate 5-lipoxygenase	ALOX5	P09917	CHEMBL215	Oxidoreductase	
Cyclooxygenase-1	PTGS1	P23219	CHEMBL221	Oxidoreductase	

Fig 11. Names and target probabilities of top 10 predicted molecular targets of curcumin obtained from Swiss TargetPrediction.

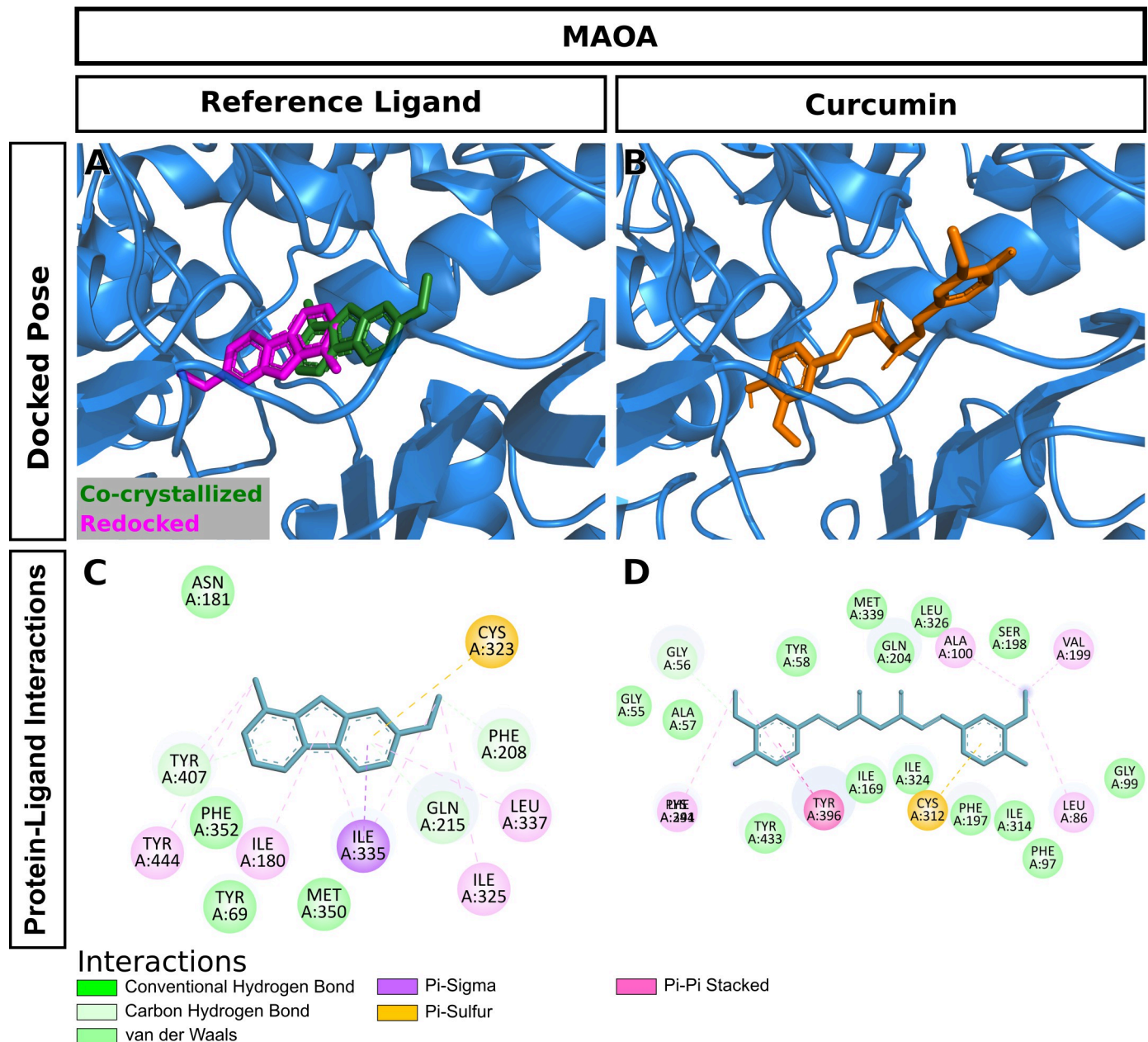https://doi.org/10.1371/journal.pone.0270123.g011

Fig 12. Molecular docking of curcumin to MAOA. (A) Redocking of the bound ligand. (B) Docking pose of curcumin. (C) Interactions of the bound ligand with the protein. (D) Predicted interactions of curcumin with the protein.

https://doi.org/10.1371/journal.pone.0270123.g012

4.1. D-gal facilitates memory impairment and mimics normal-aging in mice

In the present study, D-gal and NA mice groups exhibited less RT and FR in PA and CFC tasks, respectively (Figs 2–4). However, the RT and FR were comparable between D-gal and NA mice groups (Figs 2–4). Several studies revealed that a high dose of D-gal impairs ATP production, redox homeostasis, and increases NADPH which generates excess reactive oxygen species [10]. Other studies showed that a high ROS level could induce neuroinflammation, cellular apoptosis, and brain-derived neurotrophic factor (BDNF) dysregulation [52],
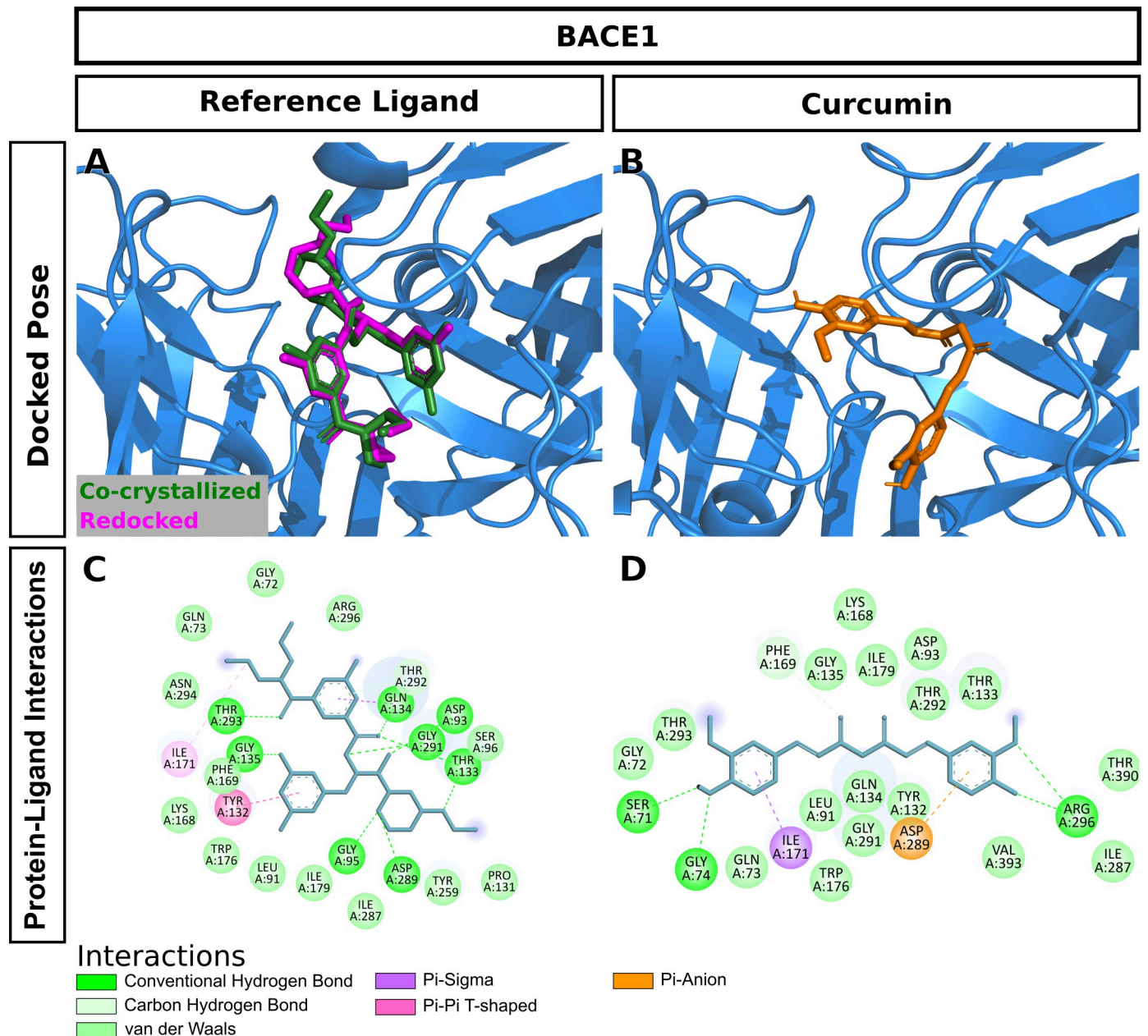
Fig 13. Molecular docking of curcumin to BACE1. (A) Redocking of the bound ligand. (B) Docking pose of curcumin. (C) Interactions of the bound ligand with the protein. (D) Predicted interactions of curcumin with the protein.

contributing to cognitive impairment. Another study showed that D-gal reduced the number of new neurons at the subgranular zone in the hippocampus area, worsening memory and the learning process in mice [53]. In addition, D-gal diminishes the expression of synaptic proteins in the hippocampus and the cerebral cortex [54]. Interestingly, D-gal-induced molecular and cellular alterations of the brain observed in experimental animals also appear during the natural progression of aging [55]. Therefore, it can be stated that D-gal mimics natural aging and draws memory deterioration in mice.

4.2. Curcumin improves D-gal and normal-aging induced memory impairment

In the current study, Curcumin + D-gal, and Curcumin + NA mice groups showed substantial protection of RT and FR in PA and CFC, respectively (Figs 2–4). The RT and FR were comparable between Curcumin + D-gal and Curcumin + NA mice groups (Figs 2–4). Moreover, curcumin was comparable to Ast, a standard antioxidant, in improving retention and freezing memory. Many studies showed that curcumin possesses anti-neuroinflammation, antioxidant and anti-aging properties [56, 57]. Another study reported that curcumin plays a protective role in brain aging by modulating cell proliferation, neuronal degeneration, and cellular senescence [14]. Therefore, it can be inferred that curcumin improves memory owing to its antioxidant and anti-aging properties in mice. Similar to previous findings [58], our study suggested that curcumin ameliorates memory impairment induced by D-gal or normal-aging in mice.

4.3. Curcumin ameliorates the oxidative biomarkers in D-gal and NA mice

In the present study, we found decreased levels of antioxidants such as GSH, SOD, and CAT (Fig 5) in D-gal and NA mice. Moreover, these levels were comparable between D-gal and NA mice (Fig 5). Many studies showed that the abnormal changes of ROS and RNS augment aging processes induced by D-gal [59] and NA [60]. In normal conditions, the antioxidant defense system comprises endogenous non-enzymatic and enzymatic compounds that counteract the deleterious effect of ROS and RNS [61]. Glutathione (GSH), a non-enzymatic antioxidant tripeptide, has a thiol group that interacts with ROS and RNS directly and reduces H_2O_2 to form H_2O [62]. In contrast, enzymatic antioxidant Superoxide Dismutase (SOD) catalyzes the dismutation of $O_2^{\bullet-}$ into H_2O_2 and O_2 [63]. Another enzymatic antioxidant, Catalase (CAT), converts H_2O_2 into H_2O and O_2; thus, cell protection from deleterious effects of H_2O_2 continues [63]. These antioxidants (GSH, SOD, CAT) prevent lipid peroxidation in the cell membrane and maintain redox homeostasis [64]. On the other hand, low levels of GSH, SOD, and CAT fail to protect against the overproduction of ROS and RNS and expedite the aging process [65].

We found a high level of AOPP, NO, and MDA in D-gal and NA mice (Fig 6), suggesting an induction of the aging process [29]. A high level of protein oxidation is known to generate excess AOPP [66]. Nitric Oxide (NO) reacts with superoxide ($O^{2\bullet-}$) to form a stronger oxidant peroxynitrite anion ($ONOO^-$). A high level of NO generates more RNS, such as $^{\bullet}NO_2$ and N_2O_3 [67], whereas an increased level of MDA promotes ROS generation [68]. Therefore, high levels of MDA, AOPP, and NO contribute to the aging process by increasing oxidative stress in the brain.

We found that both curcumin and Ast prevented the decreasing trend of GSH, SOD, and CAT levels detected in D-gal and NA groups (Fig 5), suggesting that curcumin's antioxidant activity minimized the aging-associated oxidative burden in mice [69]. Our results are also in agreement with previous studies [70].

On the other hand, substantial protection from the increasing tendency of AOPP, NO, and MDA was detected in Curcumin + D-gall and Curcumin +NA mice groups (Fig 6). These effects were comparable in the Ast group (Fig 6). Another study [71] supported these findings, suggesting that curcumin exerts its antioxidant activity by controlling the overproduction of AOPP, NO, and MDA.

4.4. Predicted interactions of curcumin with glutathione S-transferase A1, glutathione S-transferase omega-1, kelch-like ECH-associated protein 1, beta-secretase 1, and amine oxidase (flavin-containing) A to exert antioxidant activity

In our in silico studies, estimated binding energies were assessed by adopting Vina molecular docking. Estimated binding energies of curcumin with GSTA1, GSTO1, and KEAP1 were comparable with reference ligands such as Chlorambucil, C1-27, 08A, respectively (Table 2). Furthermore, curcumin is predicted to bind more strongly with GSTA1 and GSTO1 compared with the reference ligands (Table 2).

GSTA1, GSTO1, and KEAP1 are abundantly present in the hippocampus, a critical brain region crucial for hippocampus-dependent learning tasks [72, 73]. Western blot analysis showed that the upregulation of GSTA1 in the CA1 area [74] and the downregulation of GSTO1 in the hippocampus were linked to cognitive impairment, [75] commonly seen in aging animals. Other studies showed that these proteins are closely associated with oxidative stress and aging-induced neurodegenerative diseases such as memory impairment [76]. GSTA1 and GSTO1 are primary phase II detoxification enzymes and catalyze GSH conjugation in the presence of electrophile substrates [19]. Furthermore, GSTA1 suppresses the activation of c-Jun N-terminal kinase (JNK) signaling by a pro-inflammatory cytokine and oxidative stress [77]. Moreover, GSTO1 regulates the activation of interleukin-1β and stops the inflammation process in aging-associated neurodegenerative disease [20]. The Keap1-Nrf2 system plays a crucial role in regulating oxidative stress-mediated disorders [78]. A western blot analysis found a lower expression of KEAP1 in CA3 and dentate gyrus of the hippocampus under oxidative conditions [78]. The KEAP1 is closely associated with the Nrf2 cytoprotective signaling pathway and plays an antioxidative role. Under the homeostatic state, KEAP1 controls the level of Nrf2 upon binding. During stressful conditions, the KEAP1 gets oxidized in the presence of electrophile, stopping Nrf2 ubiquitylation. These cause Nrf2 to move into the nucleus forming a heterodimer with musculoaponeurotic proteins (Mafs) and initiating cytoprotective molecules such as GSH, SOD, CAT after binding with antioxidant response element (ARE) [21]. Under oxidative stress conditions, the expression of GSTA1, GSTO1, and KEAP1 are down-regulated. In contrast, the expressions are reversed upon treating with curcumin [18, 79], suggesting that curcumin is predicted to interact with GSTA1, GSTO1, and KEAP1 and potentiates the antioxidant activity.

Opposite to the down-regulation of GSTA1, GSTO1, and KEAP1, the BACE1 and MAOA proteins are elevated during the aging-associated memory impairment [80, 81]. Immunohistochemical studies showed a high level of MAOA was found in the CA3 area of the hippocampus, an important region sensitive for brain aging [82]. Studies showed that BACE1 and MAOA proteins are strongly linked to aging-associated memory impairment [22, 83]. BACE1 is widely distributed in CA1 and CA3 areas, and the absence of this protein is responsible for the altered level of synaptic plasticity in aging mice [84]. Furthermore, BACE1 plays a vital role in cleaving Aβ-peptide and causing the accumulation of amyloid-β (Aβ) peptides in the brain [85]. Likewise, MAOA produces hydrogen peroxide by oxidation of monoamine substrates in the mitochondrial outer membrane and facilitates oxidative stress [23]. We found that the estimated binding energies of curcumin upon BACE1 and MAOA were comparable with respective reference ligands (SCH734723, Harmine, respectively) (Table 2), suggesting that curcumin is predicted to interact with BACE1 and MAOA and potentiates its antioxidant role in brain aging.

5. Conclusion

We investigated the detailed effects of curcumin on oxidative stress in the D-gal and nature-induced aging mice model. Our in vivo study suggested that curcumin improves memory and rescues learning impairment by modulating oxidative stress levels. Furthermore, our in-silico study demonstrated that curcumin has good binding affinities for several molecular targets implicated in redox homeostasis. Finally, based on our in vivo and computational studies, it can be stated that curcumin improves D-gal and Normal aging-associated memory impairment by reducing oxidative overload in mice.

Supporting information

S1 Fig. Effect of curcumin on RT in D-gal and NA mice group after 48 hours of training. The RT was calculated by performing PA tasks among Vehicle, Cur-Con, D-gal, Curcumin + D-gal, Ast + D-gal, NA, Curcumin + NA, Ast + NA groups. RT was expressed in second. Data was presented as mean ± SEM, n = 8 each group; $^{****}p < 0.0001$, ns = not significant. (TIF)

S1 Data.
(XLS)

Author Contributions

Conceptualization: Md. Ashrafur Rahman, Arif Anzum Shuvo, Manik Chandra Shill, Ghazi Mohammad Sayedur Rahman, Hasan Mahmud Reza.

Data curation: Md. Ashrafur Rahman, Hasan Mahmud Reza.

Formal analysis: Md. Ashrafur Rahman, Arif Anzum Shuvo, Asim Kumar Bepari, Mehedi Hasan Apu, Manik Chandra Shill, Murad Hossain, Monjurul Kader Bakshi, Hasan Mahmud Reza.

Investigation: Md. Ashrafur Rahman, Arif Anzum Shuvo, Mehedi Hasan Apu, Murad Hossain, Monjurul Kader Bakshi.

Methodology: Md. Ashrafur Rahman, Arif Anzum Shuvo, Asim Kumar Bepari, Monjurul Kader Bakshi, Hasan Mahmud Reza.

Project administration: Md. Ashrafur Rahman, Mehedi Hasan Apu, Mohammed Uddin.

Resources: Manik Chandra Shill, Murad Hossain, Mohammed Uddin, Md. Rabiul Islam, Ghazi Mohammad Sayedur Rahman.

Software: Md. Ashrafur Rahman, Asim Kumar Bepari, Atiqur Rahman.

Supervision: Md. Ashrafur Rahman, Manik Chandra Shill, Murad Hossain, Mohammed Uddin, Javed Hasan, Hasan Mahmud Reza.

Validation: Md. Ashrafur Rahman, Mehedi Hasan Apu.

Visualization: Md. Ashrafur Rahman, Hasan Mahmud Reza.

Writing – original draft: Md. Ashrafur Rahman, Arif Anzum Shuvo, Asim Kumar Bepari, Mohammed Uddin, Md. Rabiul Islam, Javed Hasan, Ghazi Mohammad Sayedur Rahman, Hasan Mahmud Reza.

Writing – review & editing: Md. Ashrafur Rahman, Asim Kumar Bepari, Md. Rabiul Islam, Atiqur Rahman, Ghazi Mohammad Sayedur Rahman, Hasan Mahmud Reza.

References

1. López-Otín C, Blasco MA, Partridge L, Serrano M, Kroemer G. The Hallmarks of Aging. Cell. 2013; 153: 1194–1217. https://doi.org/10.1016/j.cell.2013.05.039 PMID: 23746838

2. Mattson MP, Arumugam TV. Hallmarks of Brain Aging: Adaptive and Pathological Modification by Metabolic States. Cell Metabolism. 2018; 27: 1176–1199. https://doi.org/10.1016/j.cmet.2018.05.011 PMID: 29874566

3. Lee J-S, Kim H-G, Lee H-W, Han J-M, Lee S-K, Kim D-W, et al. Hippocampal memory enhancing activity of pine needle extract against scopolamine-induced amnesia in a mouse model. Sci Rep. 2015; 5: 9651. https://doi.org/10.1038/srep09651 PMID: 25974329

4. Liu J, Wang X, Shigenaga MK, Yeo HC, Mori A, Ames BN. Immobilization stress causes oxidative damage to lipid, protein, and DNA in the brain of rats. The FASEB Journal. 1996; 10: 1532–1538. https://doi.org/10.1096/fasebj.10.13.8940299 PMID: 8940299

5. Yanar K, Aydın S, Çakatay U, Mengi M, Buyukpınarbaşılı N, Atukeren P, et al. Protein and DNA Oxidation in Different Anatomic Regions of Rat Brain in a Mimetic Ageing Model. Basic & Clinical Pharmacology & Toxicology. 2011; 109: 423–433. https://doi.org/10.1111/j.1742-7843.2011.00756.x PMID: 21733122

6. Lesné S, Koh MT, Kotilinek L, Kayed R, Glabe CG, Yang A, et al. A specific amyloid-β protein assembly in the brain impairs memory. Nature. 2006; 440: 352–357. https://doi.org/10.1038/nature04533 PMID: 16541076

7. Ullah F, Ali T, Ullah N, Kim MO. Caffeine prevents d-galactose-induced cognitive deficits, oxidative stress, neuroinflammation and neurodegeneration in the adult rat brain. Neurochemistry International. 2015; 90: 114–124. https://doi.org/10.1016/j.neuint.2015.07.001 PMID: 26209154

8. Ali T, Badshah H, Kim TH, Kim MO. Melatonin attenuates D-galactose-induced memory impairment, neuroinflammation and neurodegeneration via RAGE/NF-KB/JNK signaling pathway in aging mouse model. Journal of Pineal Research. 2015; 58: 71–85. https://doi.org/10.1111/jpi.12194 PMID: 25401971

9. Çoban J, Doğan-Ekici I, Aydın AF, Betül-Kalaz E, Doğru-Abbasoğlu S, Uysal M. Blueberry treatment decreased D-galactose-induced oxidative stress and brain damage in rats. Metab Brain Dis. 2015; 30: 793–802. https://doi.org/10.1007/s11011-014-9643-z PMID: 25511550

10. Salehpour F, Ahmadian N, Rasta SH, Farhoudi M, Karimi P, Sadigh-Eteghad S. Transcranial low-level laser therapy improves brain mitochondrial function and cognitive impairment in D-galactose–induced aging mice. Neurobiology of Aging. 2017; 58: 140–150. https://doi.org/10.1016/j.neurobiolaging.2017.06.025 PMID: 28735143

11. Yokota T, Igarashi K, Uchihara T, Jishage K, Tomita H, Inaba A, et al. Delayed-onset ataxia in mice lacking α-tocopherol transfer protein: Model for neuronal degeneration caused by chronic oxidative stress. PNAS. 2001; 98: 15185–15190. https://doi.org/10.1073/pnas.261456098 PMID: 11752462

12. Lei M, Su Y, Hua X, Ding J, Han Q, Hu G, et al. Chronic systemic injection of D-galactose impairs the septohippocampal cholinergic system in rats. NeuroReport. 2008; 19: 1611–1615. https://doi.org/10.1097/WNR.0b013e3283136a1f PMID: 18845941

13. Qu Z, Zhang J, Yang H, Huo L, Gao J, Chen H, et al. Protective effect of tetrahydropalmatine against d-galactose induced memory impairment in rat. Physiology & Behavior. 2016; 154: 114–125. https://doi.org/10.1016/j.physbeh.2015.11.016 PMID: 26592138

14. Sundaram JR, Poore CP, Sulaimee NHB, Pareek T, Cheong WF, Wenk MR, et al. Curcumin Ameliorates Neuroinflammation, Neurodegeneration, and Memory Deficits in p25 Transgenic Mouse Model that Bears Hallmarks of Alzheimer's Disease. J Alzheimers Dis. 2017; 60: 1429–1442. https://doi.org/10.3233/JAD-170093 PMID: 29036814

15. Goudarzi N, Mohammad Valipour S, Nooritahneh A, Motaghinejad M, Motevalian M, Safari S, et al. Pharmacological Evidences for Curcumin Neuroprotective Effects against Lead-Induced Neurodegeneration: Possible Role of Akt/GSK3 Signaling Pathway. Iran J Pharm Res. 2020; 19: 494–508. https://doi.org/10.22037/ijpr.2020.1101210 PMID: 33680047

16. Aggarwal S, Ichikawa H, Takada Y, Sandur SK, Shishodia S, Aggarwal BB. Curcumin (Diferuloylmethane) Down-Regulates Expression of Cell Proliferation and Antiapoptotic and Metastatic Gene Products through Suppression of IκBα Kinase and Akt Activation. Mol Pharmacol. 2006; 69: 195–206. https://doi.org/10.1124/mol.105.017400 PMID: 16219905

17. Bielak-Zmijewska A, Grabowska W, Ciolko A, Bojko A, Mosieniak G, Bijoch Ł, et al. The Role of Curcumin in the Modulation of Ageing. IJMS. 2019; 20: 1239. https://doi.org/10.3390/ijms20051239 PMID: 30871021

18. Tomobe K, Shinozuka T, Kuroiwa M, Nomura Y. Age-related changes of Nrf2 and phosphorylated GSK-3β in a mouse model of accelerated aging (SAMP8). Archives of Gerontology and Geriatrics. 2012; 54: e1–e7. https://doi.org/10.1016/j.archger.2011.06.006 PMID: 21784539

19. Tew KD, Townsend DM. Glutathione-S-Transferases As Determinants of Cell Survival and Death. Antioxidants & Redox Signaling. 2012; 17: 1728–1737. https://doi.org/10.1089/ars.2012.4640 PMID: 22540427

20. Piacentini S, Polimanti R, Squitti R, Mariani S, Migliore S, Vernieri F, et al. GSTO1*E155del polymorphism associated with increased risk for late-onset Alzheimer's disease: Association hypothesis for an uncommon genetic variant. Neuroscience Letters. 2012; 506: 203–207. https://doi.org/10.1016/j.neulet.2011.11.005 PMID: 22100662

21. Espinosa-Diez C, Miguel V, Mennerich D, Kietzmann T, Sánchez-Pérez P, Cadenas S, et al. Antioxidant responses and cellular adjustments to oxidative stress. Redox Biology. 2015; 6: 183–197. https://doi.org/10.1016/j.redox.2015.07.008 PMID: 26233704

22. Ohno M, Sametsky EA, Younkin LH, Oakley H, Younkin SG, Citron M, et al. BACE1 Deficiency Rescues Memory Deficits and Cholinergic Dysfunction in a Mouse Model of Alzheimer's Disease. Neuron. 2004; 41: 27–33. https://doi.org/10.1016/s0896-6273(03)00810-9 PMID: 14715132

23. Edmondson DE. Hydrogen peroxide produced by mitochondrial monoamine oxidase catalysis: biological implications. Curr Pharm Des. 2014; 20: 155–160. https://doi.org/10.2174/13816128113190990406 PMID: 23701542

24. Colon L, Odynocki N, Santarelli A, Poulos AM. Sexual differentiation of contextual fear responses. Learn Mem. 2018; 25: 230–240. https://doi.org/10.1101/lm.047159.117 PMID: 29661835

25. Kumar A, Prakash A, Dogra S. Protective effect of curcumin (Curcuma longa) against D-galactose-induced senescence in mice. J Asian Nat Prod Res. 2011; 13: 42–55. https://doi.org/10.1080/10286020.2010.544253 PMID: 21253949

26. Wei H, Li L, Song Q, Ai H, Chu J, Li W. Behavioural study of the d-galactose induced aging model in C57BL/6J mice. Behavioural Brain Research. 2005; 157: 245–251. https://doi.org/10.1016/j.bbr.2004.07.003 PMID: 15639175

27. Al-Amin MM, Chowdury MIA, Saifullah ARM, Alam MN, Jain P, Hossain M, et al. Levocarnitine Improves AlCl3-Induced Spatial Working Memory Impairment in Swiss albino Mice. Front Neurosci. 2019;13.

28. Pei L, Dong F, Hui B. [Effects of Astaxanthin on the damage of osteoblast induced by H2O2]. Zhongguo Gu Shang. 2008; 21: 187–189. PMID: 19105434

29. Al-Amin MdM, Reza HM, Saadi HM, Mahmud W, Ibrahim AA, Alam MM, et al. Astaxanthin ameliorates aluminum chloride-induced spatial memory impairment and neuronal oxidative stress in mice. European Journal of Pharmacology. 2016; 777: 60–69. https://doi.org/10.1016/j.ejphar.2016.02.062 PMID: 26927754

30. Tabrizian K, Yaghoobi NS, Iranshahi M, Shahraki J, Hashemzaei M. Auraptene consolidates memory, reverses scopolamine- disrupted memory in passive avoidance task, and ameliorates retention deficits in mice. Iran J Basic Med Sci. 2015; 18: 6.

31. Shoji H, Takao K, Hattori S, Miyakawa T. Contextual and Cued Fear Conditioning Test Using a Video Analyzing System in Mice. JoVE (Journal of Visualized Experiments). 2014; e50871. https://doi.org/10.3791/50871 PMID: 24637495

32. Anagnostaras SG, Josselyn SA, Frankland PW, Silva AJ. Computer-Assisted Behavioral Assessment of Pavlovian Fear Conditioning in Mice. Learn Mem. 2000; 7: 58–72. https://doi.org/10.1101/lm.7.1.58 PMID: 10706603

33. Lowry Oliver H, Rosebrough Nira J, Farr AL, Randall Rose J. PROTEIN MEASUREMENT WITH THE FOLIN PHENOL REAGENT. Journal of Biological Chemistry. 1951; 193: 265–275. https://doi.org/10.1016/S0021-9258(19)52451-6 PMID: 14907713

34. Ellman GL. Tissue sulfhydryl groups. Archives of Biochemistry and Biophysics. 1959; 82: 70–77. https://doi.org/10.1016/0003-9861(59)90090-6 PMID: 13650640

35. Al-Amin MdM, Rahman MdM, Khan FR, Zaman F, Mahmud Reza H. Astaxanthin improves behavioral disorder and oxidative stress in prenatal valproic acid-induced mice model of autism. Behavioural Brain Research. 2015; 286: 112–121. https://doi.org/10.1016/j.bbr.2015.02.041 PMID: 25732953

36. Ma L, Liu J, Li N, Wang J, Duan Y, Yan J, et al. Oxidative stress in the brain of mice caused by translocated nanoparticulate TiO2 delivered to the abdominal cavity. Biomaterials. 2010; 31: 99–105. https://doi.org/10.1016/j.biomaterials.2009.09.028 PMID: 19783296

37. Al-Amin MM, Choudhury MFR, Chowdhury AS, Chowdhury TR, Jain P, Kazi M, et al. Pretreatment With Risperidone Ameliorates Systemic LPS-Induced Oxidative Stress in the Cortex and Hippocampus. Front Neurosci. 2018;12. https://doi.org/10.3389/fnins.2018.00384

38. Sinha AK. Colorimetric assay of catalase. Analytical Biochemistry. 1972; 47: 389–394. https://doi.org/10.1016/0003-2697(72)90132-7 PMID: 4556490

39. Witko-Sarsat V, Friedlander M, Capeillère-Blandin C, Nguyen-Khoa T, Nguyen AT, Zingraff J, et al. Advanced oxidation protein products as a novel marker of oxidative stress in uremia. Kidney International. 1996; 49: 1304–1313. https://doi.org/10.1038/ki.1996.186 PMID: 8731095

40. Al-Amin MdM, Akhter S, Hasan AT, Alam T, Nageeb Hasan SM, Saifullah ARM, et al. The antioxidant effect of astaxanthin is higher in young mice than aged: a region specific study on brain. Metab Brain Dis. 2015; 30: 1237–1246. https://doi.org/10.1007/s11011-015-9699-4 PMID: 26116165

41. Tracey WR, Tse J, Carter G. Lipopolysaccharide-induced changes in plasma nitrite and nitrate concentrations in rats and mice: pharmacological evaluation of nitric oxide synthase inhibitors. J Pharmacol Exp Ther. 1995; 272: 1011–1015. PMID: 7534350

42. Niehaus WG, Samuelsson B. Formation of Malonaldehyde from Phospholipid Arachidonate during Microsomal Lipid Peroxidation. European Journal of Biochemistry. 1968; 6: 126–130. https://doi.org/10.1111/j.1432-1033.1968.tb00428.x PMID: 4387188

43. Al-Amin MdM, Hasan SMN, Alam T, Hasan AT, Hossain I, Didar RR, et al. Tadalafil enhances working memory, and reduces hippocampal oxidative stress in both young and aged mice. European Journal of Pharmacology. 2014; 745: 84–90. https://doi.org/10.1016/j.ejphar.2014.10.026 PMID: 25446565

44. Daina A, Michielin O, Zoete V. SwissTargetPrediction: updated data and new features for efficient prediction of protein targets of small molecules. Nucleic Acids Research. 2019; 47: W357–W364. https://doi.org/10.1093/nar/gkz382 PMID: 31106366

45. Pettersen EF, Goddard TD, Huang CC, Couch GS, Greenblatt DM, Meng EC, et al. UCSF Chimera—A visualization system for exploratory research and analysis. Journal of Computational Chemistry. 2004; 25: 1605–1612. https://doi.org/10.1002/jcc.20084 PMID: 15264254

46. Morris GM, Huey R, Lindstrom W, Sanner MF, Belew RK, Goodsell DS, et al. AutoDock4 and AutoDockTools4: Automated docking with selective receptor flexibility. Journal of Computational Chemistry. 2009; 30: 2785–2791. https://doi.org/10.1002/jcc.21256 PMID: 19399780

47. O'Boyle NM, Banck M, James CA, Morley C, Vandermeersch T, Hutchison GR. Open Babel: An open chemical toolbox. Journal of Cheminformatics. 2011; 3: 33. https://doi.org/10.1186/1758-2946-3-33 PMID: 21982300

48. Samdani A, Vetrivel U. POAP: A GNU parallel based multithreaded pipeline of open babel and AutoDock suite for boosted high throughput virtual screening. Computational Biology and Chemistry. 2018; 74: 39–48. https://doi.org/10.1016/j.compbiolchem.2018.02.012 PMID: 29533817

49. Schrödinger, LLC. PyMOL | pymol.org. 2015 [cited 6 Jul 2021]. Available: https://pymol.org/2/

50. Hayes JD, Flanagan JU, Jowsey IR. Glutathione Transferases. Annual Review of Pharmacology and Toxicology. 2005; 45: 51–88. https://doi.org/10.1146/annurev.pharmtox.45.120403.095857 PMID: 15822171

51. Furukawa M, Xiong Y. BTB protein Keap1 targets antioxidant transcription factor Nrf2 for ubiquitination by the Cullin 3-Roc1 ligase. Mol Cell Biol. 2005; 25: 162–171. https://doi.org/10.1128/MCB.25.1.162-171.2005 PMID: 15601839

52. Zhao W, Xu Z, Cao J, Fu Q, Wu Y, Zhang X, et al. Elamipretide (SS-31) improves mitochondrial dysfunction, synaptic and memory impairment induced by lipopolysaccharide in mice. J Neuroinflammation. 2019; 16: 230. https://doi.org/10.1186/s12974-019-1627-9 PMID: 31747905

53. Yoo DY, Kim W, Lee CH, Shin BN, Nam SM, Choi JH, et al. Melatonin improves d-galactose-induced aging effects on behavior, neurogenesis, and lipid peroxidation in the mouse dentate gyrus via increasing pCREB expression. Journal of Pineal Research. 2012; 52: 21–28. https://doi.org/10.1111/j.1600-079X.2011.00912.x PMID: 21718363

54. Wu D, Lu J, Zheng Y, Zhou Z, Shan Q, Ma D. Purple sweet potato color repairs d-galactose-induced spatial learning and memory impairment by regulating the expression of synaptic proteins. Neurobiology of Learning and Memory. 2008; 90: 19–27. https://doi.org/10.1016/j.nlm.2008.01.010 PMID: 18316211

55. Anderton BH. Ageing of the brain. Mechanisms of Ageing and Development. 2002; 123: 811–817. https://doi.org/10.1016/s0047-6374(01)00426-2 PMID: 11869738

56. Sandur SK, Ichikawa H, Pandey MK, Kunnumakkara AB, Sung B, Sethi G, et al. Role of pro-oxidants and antioxidants in the anti-inflammatory and apoptotic effects of curcumin (diferuloylmethane). Free Radical Biology and Medicine. 2007; 43: 568–580. https://doi.org/10.1016/j.freeradbiomed.2007.05.009 PMID: 17640567

57. Bala K, Tripathy BC, Sharma D. Neuroprotective and Anti-ageing Effects of Curcumin in Aged Rat Brain Regions. Biogerontology. 2006; 7: 81–89. https://doi.org/10.1007/s10522-006-6495-x PMID: 16802111

58. Banji OJF, Banji D, Ch K. Curcumin and hesperidin improve cognition by suppressing mitochondrial dysfunction and apoptosis induced by D-galactose in rat brain. Food and Chemical Toxicology. 2014; 74: 51–59. https://doi.org/10.1016/j.fct.2014.08.020 PMID: 25217884

59. Zhang J, Zheng Y, Luo Y, Du Y, Zhang X, Fu J. Curcumin inhibits LPS-induced neuroinflammation by promoting microglial M2 polarization via TREM2/ TLR4/ NF-κB pathways in BV2 cells. Mol Immunol. 2019; 116: 29–37. https://doi.org/10.1016/j.molimm.2019.09.020 PMID: 31590042

60. Jurk D, Wilson C, Passos JF, Oakley F, Correia-Melo C, Greaves L, et al. Chronic inflammation induces telomere dysfunction and accelerates ageing in mice. Nat Commun. 2014; 5: 4172. https://doi.org/10.1038/ncomms5172 PMID: 24960204

61. Souza LC, Antunes MS, Filho CB, Del Fabbro L, de Gomes MG, Goes ATR, et al. Flavonoid Chrysin prevents age-related cognitive decline via attenuation of oxidative stress and modulation of BDNF levels in aged mouse brain. Pharmacology Biochemistry and Behavior. 2015; 134: 22–30. https://doi.org/10.1016/j.pbb.2015.04.010 PMID: 25931267

62. Benzi G, Marzatico F, Pastoris O, Villa RF. Influence of oxidative stress on the age-linked alterations of the cerebral glutathione system. Journal of Neuroscience Research. 1990; 26: 120–128. https://doi.org/10.1002/jnr.490260116 PMID: 2162971

63. Weydert CJ, Cullen JJ. Measurement of superoxide dismutase, catalase and glutathione peroxidase in cultured cells and tissue. Nat Protoc. 2010; 5: 51–66. https://doi.org/10.1038/nprot.2009.197 PMID: 20057381

64. Seminotti B, Zanatta Â, Ribeiro RT, da Rosa MS, Wyse ATS, Leipnitz G, et al. Disruption of Brain Redox Homeostasis, Microglia Activation and Neuronal Damage Induced by Intracerebroventricular Administration of S-Adenosylmethionine to Developing Rats. Mol Neurobiol. 2019; 56: 2760–2773. https://doi.org/10.1007/s12035-018-1275-6 PMID: 30058022

65. Falone S, Mirabilio A, Carbone MC, Zimmitti V, Di Loreto S, Mariggiò MA, et al. Chronic exposure to 50Hz magnetic fields causes a significant weakening of antioxidant defence systems in aged rat brain. The International Journal of Biochemistry & Cell Biology. 2008; 40: 2762–2770. https://doi.org/10.1016/j.biocel.2008.05.022 PMID: 18585472

66. Choi J, Forster MJ, McDonald SR, Weintraub ST, Carroll CA, Gracy RW. Proteomic identification of specific oxidized proteins in ApoE-knockout mice: relevance to alzheimer's disease. Free Radical Biology and Medicine. 2004; 36: 1155–1162. https://doi.org/10.1016/j.freeradbiomed.2004.02.002 PMID: 15082069

67. Ridnour LA, Thomas DD, Mancardi D, Espey MG, Miranda KM, Paolocci N, et al. The chemistry of nitrosative stress induced by nitric oxide and reactive nitrogen oxide species. Putting perspective on stressful biological situations. Biological Chemistry. 2004; 385: 1–10. https://doi.org/10.1515/BC.2004.001 PMID: 14977040

68. Mecocci P, Fanó G, Fulle S, MacGarvey U, Shinobu L, Polidori MC, et al. Age-dependent increases in oxidative damage to DNA, lipids, and proteins in human skeletal muscle. Free Radical Biology and Medicine. 1999; 26: 303–308. https://doi.org/10.1016/s0891-5849(98)00208-1 PMID: 9895220

69. Rajeswari A. Curcumin protects mouse brain from oxidative stress caused by 1-methyl-4-phenyl-1,2,3,6-tetrahydropyridine. Eur Rev Med Pharmacol Sci. 2006; 10: 157–161. PMID: 16910344

70. Zaki SM, Algaleel WAA, Imam RA, Soliman GF, Ghoneim FM. Nano-curcumin versus curcumin in amelioration of deltamethrin-induced hippocampal damage. Histochem Cell Biol. 2020; 154: 157–175. https://doi.org/10.1007/s00418-020-01871-z PMID: 32227291

71. Seriner R, Dağlıoğlu K, Coşkun G, Bilgin R. Examination of the effect of curcumin in experimental liver damage created by diethylnitrosamine in swiss albino mice to superoxide dismutase and catalase activities and glutathione, malondialdehyde, advanced oxidation protein products levels. Biotechnology and Applied Biochemistry. 2021;n/a. https://doi.org/10.1002/bab.2198 PMID: 34041781

72. Rahman MA, Tanaka N, Usui K, Kawahara S. Role of Muscarinic Acetylcholine Receptors in Serial Feature-Positive Discrimination Task during Eyeblink Conditioning in Mice. PLOS ONE. 2016; 11: e0147572. https://doi.org/10.1371/journal.pone.0147572 PMID: 26808980

73. Rahman MA, Tanaka N, Nuruzzaman Md, DebNath S, Kawahara S. Blockade of the M1 muscarinic acetylcholine receptors impairs eyeblink serial feature-positive discrimination learning in mice. Sakakibara M, editor. PLoS ONE. 2020; 15: e0237451. https://doi.org/10.1371/journal.pone.0237451 PMID: 32790748

74. Landfield P, Blalock E, Chan K-C, Fossex T. Gene expression profile biomarkers and therapeutic targets for brain aging and age-related cognitive impairment. US20050071088A1, 2005. Available: https://patents.google.com/patent/US20050071088/en

75. Lee J-M, Lee JH, Song MK, Kim Y-J. NXP032 Ameliorates Aging-Induced Oxidative Stress and Cognitive Impairment in Mice through Activation of Nrf2 Signaling. Antioxidants. 2022; 11: 130. https://doi.org/10.3390/antiox11010130 PMID: 35052634

76. Wu J, Li Q, Wang X, Yu S, Li L, Wu X, et al. Neuroprotection by curcumin in ischemic brain injury involves the Akt/Nrf2 pathway. PLoS One. 2013; 8: e59843. https://doi.org/10.1371/journal.pone.0059843 PMID: 23555802

77. Romero L, Andrews K, Ng L, O'Rourke K, Maslen A, Kirby G. Human GSTA1-1 reduces c-Jun N-terminal kinase signalling and apoptosis in Caco-2 cells. Biochemical Journal. 2006; 400: 135–141. https://doi.org/10.1042/BJ20060110 PMID: 16836488

78. Yao W, Zhang J, Ishima T, Dong C, Yang C, Ren Q, et al. Role of Keap1-Nrf2 signaling in depression and dietary intake of glucoraphanin confers stress resilience in mice. Sci Rep. 2016; 6: 30659. https://doi.org/10.1038/srep30659 PMID: 27470577

79. Wu J, Ibtisham F, Niu YF, Wang Z, Li GH, Zhao Y, et al. Curcumin inhibits heat-induced oxidative stress by activating the MAPK-Nrf2 / ARE signaling pathway in chicken fibroblasts cells. Journal of Thermal Biology. 2019; 79: 112–119. https://doi.org/10.1016/j.jtherbio.2018.12.004 PMID: 30612671

80. Zhu Z, Li C, Wang X, Yang Z, Chen J, Hu L, et al. 2,2′,4′-Trihydroxychalcone from Glycyrrhiza glabra as a new specific BACE1 inhibitor efficiently ameliorates memory impairment in mice. Journal of Neurochemistry. 2010; 114: 374–385. https://doi.org/10.1111/j.1471-4159.2010.06751.x PMID: 20412384

81. Delumeau JC, Bentué-Ferrer D, Gandon JM, Amrein R, Belliard S, Allain H. Monoamine oxidase inhibitors, cognitive functions and neurodegenerative diseases. In: Tipton KF, Youdim MBH, Barwell CJ, Callingham BA, Lyles GA, editors. Amine Oxidases: Function and Dysfunction. Vienna: Springer; 1994. pp. 259–266. https://doi.org/10.1007/978-3-7091-9324-2_34 PMID: 7931235

82. Vitalis T, Fouquet C, Alvarez C, Seif I, Price D, Gaspar P, et al. Developmental expression of monoamine oxidases A and B in the central and peripheral nervous systems of the mouse. J Comp Neurol. 2002; 442: 331–347. https://doi.org/10.1002/cne.10093 PMID: 11793338

83. Singh C, Bortolato M, Bali N, Godar SC, Scott AL, Chen K, et al. Cognitive abnormalities and hippocampal alterations in monoamine oxidase A and B knockout mice. Proceedings of the National Academy of Sciences. 2013; 110: 12816–12821. https://doi.org/10.1073/pnas.1308037110 PMID: 23858446

84. Laird FM. BACE1, a Major Determinant of Selective Vulnerability of the Brain to Amyloid- Amyloidogenesis, is Essential for Cognitive, Emotional, and Synaptic Functions. Journal of Neuroscience. 2005; 25: 11693–11709. https://doi.org/10.1523/JNEUROSCI.2766-05.2005 PMID: 16354928

85. Okada H, Zhang W, Peterhoff C, Hwang JC, Nixon RA, Ryu SH, et al. Proteomic identification of sorting nexin 6 as a negative regulator of BACE1-mediated APP processing. The FASEB Journal. 2010; 24: 2783–2794. https://doi.org/10.1096/fj.09-146357 PMID: 20354142

86. Iserloh U, Wu Y, Cumming JN, Pan J, Wang LY, Stamford AW, et al. Potent pyrrolidine- and piperidine-based BACE-1 inhibitors. Bioorganic & Medicinal Chemistry Letters. 2008; 18: 414–417. https://doi.org/10.1016/j.bmcl.2007.10.116 PMID: 18023580

87. Karpusas M, Axarli I, Chiniadis L, Papakyriakou A, Bethanis K, Scopelitou K, et al. The Interaction of the Chemotherapeutic Drug Chlorambucil with Human Glutathione Transferase A1-1: Kinetic and Structural Analysis. PLOS ONE. 2013; 8: e56337. https://doi.org/10.1371/journal.pone.0056337 PMID: 23460799

88. Ramkumar K, Samanta S, Kyani A, Yang S, Tamura S, Ziemke E, et al. Mechanistic evaluation and transcriptional signature of a glutathione S -transferase omega 1 inhibitor. Nat Commun. 2016; 7: 13084. https://doi.org/10.1038/ncomms13084 PMID: 27703239

89. Ma B, Lucas B, Capacci A, Lin EY-S, Jones JH, Dechantsreiter M, et al. Design, synthesis and identification of novel, orally bioavailable non-covalent Nrf2 activators. Bioorganic & Medicinal Chemistry Letters. 2020; 30: 126852. https://doi.org/10.1016/j.bmcl.2019.126852 PMID: 31898999

90. Son S-Y, Ma J, Kondou Y, Yoshimura M, Yamashita E, Tsukihara T. Structure of human monoamine oxidase A at 2.2-Å resolution: The control of opening the entry for substrates/inhibitors. PNAS. 2008; 105: 5739–5744. https://doi.org/10.1073/pnas.0710626105 PMID: 18391214